

# A New Approach to the Modeling and Analysis of Fracture through Extension of Continuum Mechanics to the Nanoscale

T. SENDOVA

*Institute for Mathematics and Its Applications, University of Minnesota, Minneapolis, MN 55403, USA*

J. R. WALTON

*Department of Mathematics, Texas A&M University, College Station, TX 77843-3368, USA*

*Abstract:* In this paper we focus on the analysis of the partial differential equations arising from a new approach to modeling brittle fracture based on an extension of continuum mechanics to the nanoscale. It is shown that ascribing constant surface tension to the fracture surfaces and using the appropriate crack surface boundary condition given by the jump momentum balance leads to a sharp crack opening profile at the crack tip but predicts logarithmically singular crack tip stress. However, a modified model, where the surface excess property is responsive to the curvature of the fracture surfaces, yields bounded stresses and a cusp-like opening profile at the crack tip. Further, two possible fracture criteria in the context of the new theory are discussed. The first is an energy-based crack growth condition, while the second employs the finite crack tip stress the model predicts. The classical notion of energy release rate is based upon the singular solution, whereas for the modeling approach adopted here, a notion analogous to the energy release rate arises through a different mechanism associated with the rate of working of the surface excess properties at the crack tip.

*Key Words:* fracture, surface excess properties, fracture criteria

## 1. INTRODUCTION

### *1.1. Fracture Mechanics: Continuum to Atomistic Approaches*

Fracture of brittle materials has been modeled over a broad range of approaches: from classical continuum theories such as linear elastic fracture mechanics (LEFM) to particulate theories such as molecular dynamics.

Various attempts have been made to supplement the classical continuum approaches so that the internal inconsistencies in the LEFM theory are circumvented. Cohesive and process zone models are among the most widely studied generalizations of the classical

crack tip model. These types of models require the specification of constitutive properties of the cohesive or crack tip process zone, which are very difficult to determine experimentally. Thus, the models used are either based on *ad hoc* choices for the constitutive behavior of the cohesive/process zone or on simplified views of the fracture process.<sup>1</sup>

The primary motivation for studying fracture through atomistic scales, in addition to the fact that they take into account the nanoscale interfacial physics that plays a crucial role in a neighborhood of the fracture edge, is that the classical continuum models do not contain the necessary physics to predict fracture. In this sense, molecular dynamics offers an appealing approach to studying the initiation and propagation of fracture, which explains the growing literature devoted to this technique [4–11]. On the other hand, it requires an accurate description of the long-range and short-range intermolecular forces in the bulk material, which is a difficult task in the case of liquids and solids [8].

Various multiscale models (so-called *atom-to-continuum modeling*) have also recently gained considerable attention. One of the most extensively studied methods of this type, in the context of finite-element method (FEM) approximations to continuum models, is the quasi-continuum method introduced by Tadmor et al. [12]. Based on an atomistic view of material behavior, its continuum aspect comes from the fact that the FEM is based on energy minimization. A different type of atom-to-continuum modeling is a recently proposed approach by Xiao and Belytschko [13] which involves the introduction of *bridging domains* between regions modeled using bulk (continuum) descriptions of material behavior and regions modeled using atomistic descriptions of material behavior. Both of these approaches involve adjustable parameters that one needs to fit for every particular application.

Other attempts to incorporate microscale processes into fracture modeling include models based on configurational forces, as considered by Gurtin and Podio-Guidugli [14, 15], Gurtin and Shvartsman [16], Sivaloganathan and Spector [17], Maugin and Trimarco [18], Fomethé and Maugin [19] and others. Also gaining attention is the peridynamic paradigm for modeling fracture [20].

In contrast to the latter theories, which introduce either an entirely new additional force system (configurational forces) or an entirely new continuum modeling paradigm (peridynamics), the theory proposed herein uses conventional ideas of continuum mechanics through the introduction of a dividing surface endowed with excess properties together with a mutual force. Our approach builds upon a hybrid theory introduced by Oh et al. [21]. Unlike a start-from-scratch atom-to-continuum approach, this theory is based on a continuum theory of material behavior that takes into account effects due to long-range intermolecular forces from adjoining phases in the vicinity of the fracture surfaces. No adjustable parameters are needed and, as demonstrated in Section 4, the theory using curvature-dependent surface tension predicts a finite crack tip stress amplification of the applied loading, in contrast to the crack tip stress singularity exhibited by models in classical elastic fracture mechanics. This allows us to formulate a fracture criterion based upon the notion of a *critical crack tip stress* (CCTS) defined to be the minimum crack tip stress level required to propagate the crack in addition to an energy-based crack growth condition similar to the classical notion of a critical energy release rate (ERR) defined in the setting of singular crack tip stresses and strains.

### 1.2. Current versus Reference Configuration

Classical fracture theories are customarily formulated in a reference configuration. However, aspects of the theory discussed here are more easily described in the current or deformed configuration. For example, the correction potential, which determines the mutual body force term and, depending on the model, the crack surface excess properties, is set up only when chemical bonds have been broken and depends on the crack opening profile.

On the other hand, formulating a fracture theory in the current configuration presents certain complications. First, it is not entirely clear how one should mathematically define a fracture in the deformed configuration, where the crack is opened, as traditionally a crack is defined as a surface in the reference configuration across which the displacement, velocity, stress fields, etc. could sustain a discontinuity. Also, the notions of crack length and crack velocity in the current configuration are ambiguous, since one needs to separate *crack tip motion due to crack growth* from *motion due to deformation*. (A convenient method for doing this is presented below in Section 5.) Furthermore, to prove that the proposed modeling approach leads to bounded stresses and strains, we employ the method of integral transforms which is most easily applied when using the undeformed configuration as a reference.

## 2. PRELIMINARY DEFINITIONS

The notation introduced in this section is common to both the quasi-static and the dynamic cases. In Section 4 attention is limited to studying the boundary-value problem arising when considering a classical (quasi-static) Griffith crack. In this case, time is just a parameter and does not affect the mechanics, for this reason the time dependence is often suppressed in the notation. When deriving an energy-based crack growth condition in Section 5, a dynamic problem needs to be considered.

With subscript  $\kappa$  we denote quantities defined relative to a natural reference (unloaded) configuration. The material body in the reference configuration is denoted by  $\mathcal{B}_\kappa(t)$ , where the time dependence is due to (possible) crack extension (Section 5). Here  $\mathcal{B}_\kappa(t)$  is viewed as an *evolving reference configuration*. The boundary of  $\mathcal{B}_\kappa(t)$ , denoted by  $\partial\mathcal{B}_\kappa(t)$ , has the decomposition

$$\partial\mathcal{B}_\kappa(t) = \mathcal{S}_\kappa \cup \Sigma_\kappa(t) \quad (1)$$

where  $\mathcal{S}_\kappa$  denotes the boundary the body would have in the absence of the crack (which does not evolve with time) and  $\Sigma_\kappa(t)$  denotes the crack. The location of the crack tip in the reference configuration is denoted by  $\mathbf{c}(t)$  (Figure 1). To that end,  $\dot{\mathbf{c}}(t)$  is the *crack extension velocity*.

Let  $\mathbf{X}$  denote the position of points in  $\mathcal{B}_\kappa(t)$ , and  $\chi(\mathbf{X}, t)$ ,  $\mathbf{X} \in \mathcal{B}_\kappa(t)$  a motion of the cracked body which might be accompanied by crack extension. The body, its boundary sets and the crack tip in the current (deformed) configuration are denoted by  $\mathcal{B}_t$ ,  $\mathcal{S}_t$ ,  $\Sigma_t$ , and  $\mathbf{c}_t$ , respectively.<sup>2</sup> Spatial points are denoted by  $\mathbf{x} \in \mathcal{B}_t$ . The material and spatial descriptions of the displacement are denoted by  $\mathbf{u}_\kappa(\mathbf{X}, t) (:= \chi(\mathbf{X}, t) - \mathbf{X})$  and  $\mathbf{u}(\mathbf{x}, t)$ , respectively, and  $\mathbf{v}(\mathbf{x}, t)$  is the spatial description of the velocity. Let  $\mathbf{F}(\mathbf{X}, t)$  denote the deformation gradient

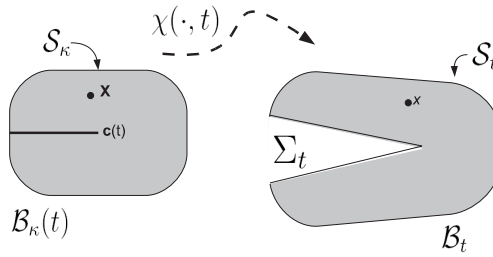


Figure 1. Edge crack in the reference and current configurations.

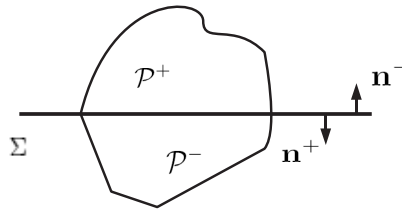


Figure 2. Part  $\mathcal{P}$  of a body, intersecting the dividing surface  $\Sigma$ .

and let  $J = \det(\mathbf{F})$ . The gradient and divergence operators are denoted by  $\text{grad}$  and  $\text{div}$  in the spatial frame, and by  $\nabla$  and  $\text{Div}$  in the material frame. Similarly, surface gradient and surface divergence are denoted by  $\text{grad}_{(\sigma)}$  and  $\text{div}_{(\sigma)}$  and by  $\nabla_{(\sigma)}$  and  $\text{Div}_{(\sigma)}$  in the spatial and material frame, respectively.<sup>3</sup>

If  $\mathbf{s}_\kappa$  is an oriented curve in the fracture surface  $\Sigma_\kappa(t)$ , parameterized by arc length  $S \in (0, L)$ ,  $\mathbf{v}_\kappa$  denotes the *unit conormal vector* to  $\mathbf{s}_\kappa$ , i.e.  $\mathbf{v}_\kappa = \boldsymbol{\tau}_\kappa \times \mathbf{N}$ , where  $\mathbf{N}$  is the unit normal to  $\Sigma_\kappa(t)$  and  $\boldsymbol{\tau}_\kappa = \frac{d\mathbf{s}_\kappa}{dS}$  is the unit tangent to  $\mathbf{s}_\kappa$ .

Let  $\mathcal{P}$  be a part of the body intersecting the dividing surface  $\Sigma$ . Let  $\mathcal{P}^+$  denote the domain occupied by the first phase (e.g. bulk material) and  $\mathcal{P}^-$  be the domain occupied by the second (e.g. gas or vacuum). Then  $\mathcal{P} = \mathcal{P}^+ \cup (\Sigma \cap \mathcal{P}) \cup \mathcal{P}^-$  (Figure 2). Let the limit of a generic bulk field  $\phi(\mathbf{x})$  in  $\mathcal{P} \setminus \Sigma$  be defined by

$$\phi^\pm(\mathbf{x}) := \lim_{s \rightarrow 0^+} \phi(\mathbf{x} - s\mathbf{n}^\pm) \quad \text{for all } \mathbf{x} \in \Sigma$$

where  $\mathbf{n}^\pm$  is the outward (for  $\mathcal{P}^\pm$ ) unit normal vector to the dividing surface  $\Sigma$ . Given a field  $\phi(\mathbf{x})$  we define the jump of  $\phi$  across  $\Sigma$  by

$$\llbracket \phi \rrbracket := \phi^+ - \phi^-.$$

Similarly, for a field  $\phi^{(\sigma)}(\mathbf{x})$ , defined on the fracture surfaces,

$$(\phi^{(\sigma)}\mathbf{v}) := \phi^{(\sigma,+)}\mathbf{v}^+ + \phi^{(\sigma,-)}\mathbf{v}^-$$

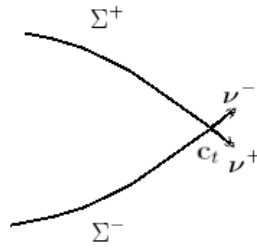


Figure 3. The  $\mathbf{v}^+$  and  $\mathbf{v}^-$  - unit tangent vectors to  $\Sigma^+$  and  $\Sigma^-$ , respectively, and normal to the crack edge  $\mathbf{c}_t$ .

denotes the jump of  $\phi^{(\sigma)}\mathbf{v}$  at the crack edge. Here

$$\phi^{(\sigma,\pm)}(\mathbf{c}_t) := \lim_{s \rightarrow 0^+} \phi^{(\sigma)}(\mathbf{c}_t - s\mathbf{v}^\pm)$$

and  $\mathbf{v}^\pm$  is the unit conormal vector to the crack edge  $\mathbf{c}_t$  (tangent to the crack surface  $\Sigma^\pm$  and, in three dimensions, normal to  $\mathbf{c}_t$ ), pointing away from the fracture surfaces (Figure 3).

Let  $\mathbf{T}$  denote the Cauchy stress tensor and  $\mathbf{T}_\kappa$  – the first Piola–Kirchhoff stress tensor. Further, let the matrix representation of the first Piola–Kirchhoff stress tensor in Cartesian coordinates be given by

$$[\mathbf{T}_\kappa] = \begin{pmatrix} \sigma_{11} & \sigma_{12} \\ \sigma_{12} & \sigma_{22} \end{pmatrix}.$$

We assume that there exists a surface Cauchy stress tensor  $\mathbf{T}^{(\sigma)}$  which gives contact forces on a curve in the fracture surface  $\Sigma$ . For simplicity and consistency with the literature [22, p. 148] assume that the surface stress can be modeled as Eulerian, i.e.  $\mathbf{T}^{(\sigma)} = \tilde{\gamma}\mathbf{P}_t$ . Here  $\mathbf{P}_t$  is the perpendicular projection onto the tangent space  $\mathcal{T}_x$  to  $\Sigma_t$  at  $\mathbf{x}$ . We refer to  $\tilde{\gamma}$  as the *surface tension*. Further, let  $H$  denote the mean curvature (see (79), Appendix A).

### 3. FORMULATION OF THE PROBLEM IN THE REFERENCE CONFIGURATION

We consider a classical Griffith crack, meaning a static, mode I crack of finite length in an infinite linear elastic body, subjected to far-field tensile loading  $\sigma$ .

In view of the fact that the method of integral transforms is most easily applied when the problem is formulated in a reference configuration where the crack is just a slit, we work in the unloaded configuration of the body.

In order to simplify the presentation, assume that  $\mathbf{X} = \langle X_1, X_2 \rangle$  is non-dimensionalized by crack length, so that the crack in the reference configuration is parameterized by

$$\Sigma_{\kappa}^{\pm} = \{\mathbf{X} : -1 \leq X_1 \leq 1, X_2 = 0^{\pm}\}.$$

Consequently, in the current configuration, the upper/lower crack surface can be parameterized by

$$\Sigma^{\pm} = \{\mathbf{x} : x_1 = X_1 + u_1(X_1, 0^{\pm}), x_2 = u_2(X_1, 0^{\pm}), -1 \leq X_1 \leq 1\} \quad (2)$$

where  $\mathbf{x} = \langle x_1, x_2 \rangle$  and  $\langle u_1, u_2 \rangle$  are the components of  $\mathbf{u}_{\kappa}(\mathbf{X})$ .

Let  $\mathcal{P}_{\kappa} \subset \mathcal{B}_{\kappa}$  be a part in the reference configuration of the body and let  $\mathcal{P} = \chi(\mathcal{P}_{\kappa})$ . Then, provided that  $\mathcal{P}$  does not contain the fracture tip, the force acting on  $\mathcal{P}$  is

$$\begin{aligned} \mathcal{F}(\mathcal{P}) &= \int_{\partial\mathcal{P}} \mathbf{T}\mathbf{n} \, da + \int_{\mathcal{P}} \mathbf{b} \, dv + \int_{\partial(\Sigma \cap \mathcal{P})} \mathbf{T}^{(\sigma)}\mathbf{v} \, ds \\ &= \int_{\partial\mathcal{P}} \mathbf{T}\mathbf{n} \, da + \int_{\mathcal{P}} \mathbf{b} \, dv + \int_{\Sigma \cap \mathcal{P}} \operatorname{div}_{(\sigma)} \mathbf{T}^{(\sigma)} \, da \\ &= \int_{\partial\mathcal{P}_{\kappa}} J \mathbf{T}_m \mathbf{F}^{-T} \mathbf{N} \, dA + \int_{\mathcal{P}_{\kappa}} J \mathbf{b} \, dV \\ &\quad + \int_{\Sigma_{\kappa} \cap \mathcal{P}_{\kappa}} J (\operatorname{div}_{(\sigma)} \mathbf{T}^{(\sigma)} \otimes \mathbf{n}^-)_m \mathbf{F}^{-T} \mathbf{N}^- \, dA \end{aligned} \quad (3)$$

where  $\mathbf{b}$  is the mutual body force term in the current configuration,  $\mathbf{n}$  is the outward unit normal vector to  $\partial\mathcal{P}$  and  $\mathbf{n}^-$  is the unit normal to the crack profile  $\Sigma$  pointing into the bulk material,  $\mathbf{N}$  is the outward unit normal vector to  $\partial\mathcal{P}_{\kappa}$  and  $\mathbf{N}^-$  is the unit normal to the reference crack profile  $\Sigma_{\kappa}$  pointing into the bulk material,  $\mathbf{v}$  is the conormal to  $\partial(\Sigma \cap \mathcal{P})$ , while  $\mathbf{T}_m$  is the material description of  $\mathbf{T}$ , i.e.  $\mathbf{T}_m(\mathbf{X}) = \mathbf{T}(\chi(\mathbf{X}))$ . If the fracture tip  $\mathbf{c}$  is in  $\mathcal{P}$ , then there is an additional contribution to  $\mathcal{F}(\mathcal{P})$  due to the excess properties at the crack tip, namely

$$\begin{aligned} \mathcal{F}(\mathcal{P}) &= \int_{\partial\mathcal{P}} \mathbf{T}\mathbf{n} \, da + \int_{\mathcal{P}} \mathbf{b} \, dv + \int_{\partial(\Sigma \cap \mathcal{P})} \mathbf{T}^{(\sigma)}\mathbf{v} \, ds + \mathbf{b}^{(c)} \\ &= \int_{\partial\mathcal{P}} \mathbf{T}\mathbf{n} \, da + \int_{\mathcal{P}} \mathbf{b} \, dv + \int_{\Sigma \cap \mathcal{P}} \operatorname{div}_{(\sigma)} \mathbf{T}^{(\sigma)} \, da - (\mathbf{T}^{(\sigma)}\mathbf{v})(\mathbf{c}_t) + \mathbf{b}^{(c)} \\ &= \int_{\partial\mathcal{P}_{\kappa}} J \mathbf{T}_m \mathbf{F}^{-T} \mathbf{N} \, dA + \int_{\mathcal{P}_{\kappa}} J \mathbf{b} \, dV \\ &\quad + \int_{\Sigma_{\kappa} \cap \mathcal{P}_{\kappa}} J (\operatorname{div}_{(\sigma)} \mathbf{T}^{(\sigma)} \otimes \mathbf{n}^-)_m \mathbf{F}^{-T} \mathbf{N}^- \, dA - (\mathbf{T}_{\kappa}^{(\sigma)}\mathbf{v}_{\kappa})(\mathbf{c}) + \mathbf{b}_{\kappa}^{(c)} \end{aligned} \quad (4)$$

where  $\mathbf{b}^{(c)}$  is a mutual force acting at the crack tip, arising due to resistance of chemical bonds to opening of the fracture surfaces at the fracture tip and  $\mathbf{b}_{\kappa}^{(c)}$  is the corresponding

body force in the reference configuration. Here we have used that in the case of plane strain  $\|\mathbf{F}(\mathbf{c})\boldsymbol{\tau}_\kappa(\mathbf{c})\| = 1$ , which in turn implies  $\mathbf{b}^{(c)} = \mathbf{b}_\kappa^{(c)}$ . Recall that the first Piola–Kirchhoff stress tensor is given by

$$\mathbf{T}_\kappa = J\mathbf{T}_m\mathbf{F}^{-T}.$$

Let  $\mathbf{b}_\kappa$  denote the body force in the reference configuration, then  $\mathbf{b}_\kappa = J\mathbf{b}$ . Using

$$\int_{\partial\mathcal{P}_\kappa} \mathbf{T}_\kappa\mathbf{N} dA = \int_{\mathcal{P}_\kappa} \text{Div}\mathbf{T}_\kappa dV + \int_{\Sigma_\kappa\cap\mathcal{P}_\kappa} \llbracket\mathbf{T}_\kappa\rrbracket\mathbf{N}^- dA, \tag{5}$$

we transform (4) to

$$\begin{aligned} \mathcal{F}(\mathcal{P}) &= \int_{\mathcal{P}_\kappa} (\text{Div}\mathbf{T}_\kappa + \mathbf{b}_\kappa) dV \\ &+ \int_{\Sigma_\kappa\cap\mathcal{P}_\kappa} (J(\text{div}_{(\sigma)}\mathbf{T}^{(\sigma)} \otimes \mathbf{n}^-)_m\mathbf{F}^{-T}\mathbf{N}^- + \llbracket\mathbf{T}_\kappa\rrbracket\mathbf{N}^-) dA \\ &- (\mathbf{T}_\kappa^{(\sigma)}\mathbf{v}_\kappa)(\mathbf{c}) + \mathbf{b}_\kappa^{(c)}. \end{aligned} \tag{6}$$

If  $\mathbf{c}_t \notin \mathcal{P}$ , the last two terms in (6) should not be included in  $\mathcal{F}(\mathcal{P})$ . Since equilibrium requires  $\mathcal{F}(\mathcal{P}) = \mathbf{0}$ , application of the localization theorem to the first term in (6) implies that the differential momentum balance in the reference configuration can be expressed as

$$\text{Div}\mathbf{T}_\kappa + \mathbf{b}_\kappa = \mathbf{0}, \tag{7}$$

the jump momentum balance<sup>4</sup> by

$$J(\text{div}_{(\sigma)}\mathbf{T}^{(\sigma)} \otimes \mathbf{n}^-)_m\mathbf{F}^{-T}\mathbf{N}^- + \llbracket\mathbf{T}_\kappa\rrbracket\mathbf{N}^- = \mathbf{0}, \tag{8}$$

and the crack tip momentum balance by

$$\mathbf{b}_\kappa^{(c)} = (\mathbf{T}_\kappa^{(\sigma)}\mathbf{v}_\kappa)(\mathbf{c}). \tag{9}$$

The jump momentum balance in Cartesian component form is

$$\begin{aligned} \sigma_{12} &= -\frac{(1 + u_{1,1})^2 + u_{1,2}u_{2,1}}{\sqrt{(1 + u_{1,1})^2 + u_{2,1}^2}} \left( \frac{\tilde{\gamma}'(x_1)(1 + u_{1,1})^2}{(1 + u_{1,1})^2 + u_{2,1}^2} \right. \\ &+ \left. \frac{\tilde{\gamma}u_{2,1}(u_{2,1}^2u_{1,12} + u_{2,1}(1 + u_{1,1})(u_{1,11} - u_{2,12}) - (1 + u_{1,1})^2u_{2,11})}{((1 + u_{1,1})^2 + u_{2,1}^2)^2} \right) \end{aligned}$$

$$\sigma_{22} = -\frac{(1 + u_{1,1})^2 + u_{1,2}u_{2,1}}{\sqrt{(1 + u_{1,1})^2 + u_{2,1}^2}} \left( \frac{\tilde{\gamma}'(x_1)(1 + u_{1,1})u_{2,1}}{(1 + u_{1,1})^2 + u_{2,1}^2} - \frac{\tilde{\gamma}(1 + u_{1,1})(u_{2,1}^2 u_{1,12} + u_{2,1}(1 + u_{1,1})(u_{1,11} - u_{2,12}) - (1 + u_{1,1})^2 u_{2,11})}{((1 + u_{1,1})^2 + u_{2,1}^2)^2} \right), \quad (10)$$

where  $u_{i,j} = \frac{\partial u_i}{\partial x_j}$ . A detailed derivation of Equations (10) is provided in Appendix B. The jump momentum balance provides boundary conditions on the crack surfaces which are highly non-linear because of the ascribed surface excess properties. Owing to symmetry, it suffices to consider the problem on the upper half plane only. In this case, additional boundary conditions are needed on  $\{\mathbf{X} : |X_1| > 1, X_2 = 0\}$ . Symmetry implies

$$\begin{aligned} u_2(X_1, 0) &= 0, \quad |X_1| > 1 \\ \sigma_{12}(X_1, 0) &= 0, \quad |X_1| > 1. \end{aligned} \quad (11)$$

We assume that the constitutive behavior of the material can be modeled by Hooke's law in the reference configuration, that is, the Piola–Kirchhoff stress tensor  $\mathbf{T}_\kappa$  is given by

$$\mathbf{T}_\kappa = 2\mu\mathbf{E} + \lambda\text{tr}(\mathbf{E})\mathbf{I} \quad (12)$$

where

$$\mathbf{E} = \frac{1}{2}(\nabla\mathbf{u}_\kappa + \nabla\mathbf{u}_\kappa^T)$$

is the infinitesimal strain tensor and  $\lambda$  and  $\mu$  are the *Lamé moduli*.

Also, a homogeneous tensile far-field loading is assumed, i.e.

$$\begin{aligned} \lim_{X_2 \rightarrow \infty} \sigma_{11}(X_1, X_2) &= 0 \\ \lim_{X_2 \rightarrow \infty} \sigma_{12}(X_1, X_2) &= 0 \\ \lim_{X_2 \rightarrow \infty} \sigma_{22}(X_1, X_2) &= \sigma. \end{aligned} \quad (13)$$

Thus, the problem we are going to consider is formulated in the reference configuration (the upper half plane) and consists of:

1. a differential momentum balance given by Equation (7);
2. boundary conditions on  $\{\mathbf{X} : |X_1| \leq 1, X_2 = 0\}$  given by the jump momentum balance, Equations (10);
3. boundary conditions on  $\{\mathbf{X} : |X_1| > 1, X_2 = 0\}$  given by Equations (11);
4. a constitutive equation given by Equation (12);
5. a far filed loading condition given by Equation (13).

**4. METHOD OF INTEGRAL TRANSFORMS APPLIED TO THE NAVIER EQUATIONS**

**4.1. Model with Constant Surface Tension and Zero Mutual Body Force Term**

As a first step in our analysis we consider a model with constant surface tension ( $\tilde{\gamma} \equiv \text{const}$ ) and zero mutual body force, i.e.  $\mathbf{b}_x = \mathbf{0}$  in (7). The method of integral transforms applied to the Navier equations is used, a key step in which is the construction of the so-called *Dirichlet-to-Neumann* and *Neumann-to-Dirichlet maps*, derived in Appendix A. For the model with no mutual body force correction term, the Dirichlet-to-Neumann and Neumann-to-Dirichlet maps reduce, respectively, to

$$\begin{aligned} \sigma_{12}(x, 0) &= \frac{2\mu^2}{\lambda + 3\mu} u_{2,1}(x, 0) + \frac{2\mu(\lambda + 2\mu)}{(\lambda + 3\mu)\pi} \int_{-\infty}^{\infty} \frac{u_{1,1}(r, 0)}{r - x} dr \\ \sigma_{22}(x, 0) &= -\frac{2\mu^2}{\lambda + 3\mu} u_{1,1}(x, 0) + \frac{2\mu(\lambda + 2\mu)}{(\lambda + 3\mu)\pi} \int_{-\infty}^{\infty} \frac{u_{2,1}(r, 0)}{r - x} dr \end{aligned} \tag{14}$$

and

$$\begin{aligned} u_{1,1}(x, 0) &= -\frac{\lambda + 2\mu}{2\mu(\lambda + \mu)\pi} \int_{-\infty}^{\infty} \frac{\sigma_{12}(r, 0)}{r - x} dr + \frac{1}{2(\lambda + \mu)} \sigma_{22}(x, 0) \\ u_{2,1}(x, 0) &= -\frac{\lambda + 2\mu}{2\mu(\lambda + \mu)\pi} \int_{-\infty}^{\infty} \frac{\sigma_{22}(r, 0)}{r - x} dr - \frac{1}{2(\lambda + \mu)} \sigma_{12}(x, 0) \end{aligned} \tag{15}$$

where  $\int$  denotes a Cauchy principal value integral. For simplicity, in this section, the indicial notation  $(X_1, X_2)$  has been replaced by  $(x, y)$ . Substituting the first equation of (15) into the second of (14) and using the boundary conditions (11) on  $|x| > 1$ , one arrives at

$$\begin{aligned} \sigma_{22}(x, 0) &= \frac{2\mu(\lambda + \mu)}{(\lambda + 2\mu)\pi} \int_{-1}^1 \frac{u_{2,1}(r, 0)}{r - x} dr + \frac{\mu}{(\lambda + 2\mu)\pi} \int_{-1}^1 \frac{\sigma_{12}(r, 0)}{r - x} dr \\ &= \frac{E}{2(1 - \nu^2)\pi} \int_{-1}^1 \frac{u_{2,1}(r, 0)}{r - x} dr + \frac{1 - 2\nu}{2(1 - \nu)\pi} \int_{-1}^1 \frac{\sigma_{12}(r, 0)}{r - x} dr. \end{aligned} \tag{16}$$

Here  $E$  and  $\nu$  denote Young’s modulus and Poisson’s ratio, respectively:

$$E = \frac{\mu(3\lambda + 2\mu)}{\lambda + \mu}, \quad \nu = \frac{\lambda}{2(\lambda + \mu)}.$$

We now linearize the jump momentum balance boundary conditions (10) under the assumption that  $u_{i,j}(x, 0)$  and  $u_{i,jk}(x, 0)$  are small. The solution of the linearized problem will then be checked for consistency with the assumptions made.

From (10) it is evident that the asymptotic form of the jump momentum balance equations is

$$\begin{aligned}\sigma_{12}(x, 0) &= 0 + \text{h.o.t.}, \quad |x| \leq 1 \\ \sigma_{22}(x, 0) &= -\tilde{\gamma} u_{2,11}(x, 0) + \text{h.o.t.}, \quad |x| \leq 1\end{aligned}\quad (17)$$

where ‘h.o.t.’ denotes higher order terms.

Let  $\hat{u}$  denote the Fourier transform of  $u$  with respect to the  $x$  variable. Note that<sup>5</sup> the Dirichlet-to-Neumann and the Neumann-to-Dirichlet maps (and, consequently, Equation (16)) were derived under the assumption that  $\hat{u}_{1,1}(p, y)$  and  $\hat{u}_{2,1}(p, y)$  vanish in the limit as  $y \rightarrow \infty$ , whereas the far-field loading condition for our problem is given by (13). In order to reduce the considered problem to a problem which satisfies the above assumptions, we use the linearity of the differential momentum balance and the (linearized) boundary conditions and introduce  $\mathbf{u}^f$  and  $\mathbf{u}^0$  such that  $\mathbf{u}_\kappa = \mathbf{u}^f + \mathbf{u}^0$  with  $\mathbf{u}^f$  being the displacement field corresponding to the homogeneous stress field

$$\mathbf{T}_\kappa^f = \begin{pmatrix} 0 & 0 \\ 0 & \sigma \end{pmatrix}. \quad (18)$$

Since the stress and strain tensors corresponding to  $\mathbf{u}^f$  are related constitutively by Hooke’s law, i.e.  $\mathbf{T}_\kappa^f = 2\mu\mathbf{E}^f + \lambda\text{tr}(\mathbf{E}^f)\mathbf{I}$ , where  $\mathbf{E}^f = \frac{1}{2}(\nabla\mathbf{u}^f + (\nabla\mathbf{u}^f)^T)$ , one easily finds

$$\begin{aligned}u_1^f(x, y) &= -\frac{\lambda\sigma}{4\mu(\lambda + \mu)}x \\ u_2^f(x, y) &= \frac{(\lambda + 2\mu)\sigma}{4\mu(\lambda + \mu)}y.\end{aligned}\quad (19)$$

The stress corresponding to  $\mathbf{u}^0$  vanishes in the limit as  $y \rightarrow \infty$ , and consequently

$$\lim_{y \rightarrow \infty} \hat{u}_{1,1}^0(p, y) = 0 \quad \text{and} \quad \lim_{y \rightarrow \infty} \hat{u}_{2,1}^0(p, y) = 0$$

that is,  $\mathbf{u}^0$  satisfies the assumptions under which Equation (16) was derived.

From the definition of  $\mathbf{u}^0$  and Equations (17) and (18) one concludes that

$$\begin{aligned}\sigma_{12}^0(x, 0) &= 0 + \text{h.o.t.}, \quad |x| \leq 1 \\ \sigma_{22}^0(x, 0) &= -\sigma - \tilde{\gamma} u_{2,11}(x, 0) + \text{h.o.t.}, \quad |x| \leq 1.\end{aligned}\quad (20)$$

Substituting the above equations into (16) one arrives at

$$-\sigma - \tilde{\gamma} u_{2,11}^0(x, 0) = \frac{E}{2(1 - \nu^2)\pi} \int_{-1}^1 \frac{u_{2,1}^0(r, 0)}{r - x} dr. \quad (21)$$

Let us define

Table 1. Values of  $u_{2,1}(1, 0)$  for various values of the (non-dimensional) far-field loading  $\sigma$  and (non-dimensional) excess property  $\tilde{\gamma}$ .

$\tilde{\gamma}$	$\sigma$	$u_{2,1}(1, 0)$
0.05	0.001	-0.0069
	0.002	-0.0139
	0.004	-0.0278
0.1	0.001	-0.0046
	0.002	-0.0093
	0.004	-0.0185
0.2	0.001	-0.0030
	0.002	-0.0059
	0.004	-0.0119

$$\phi(x) = u_{2,1}^0(x, 0), \quad \zeta = \frac{E}{2(1 - \nu^2)}. \tag{22}$$

Then Equation (21) takes the form

$$\tilde{\gamma} \phi'(x) + \frac{\zeta}{\pi} \int_{-1}^1 \frac{\phi(r)}{r - x} dr = -\sigma, \quad x \in [-1, 1]. \tag{23}$$

This is a Cauchy singular, linear integro-differential equation. It arises, for example, when modeling combined infrared gaseous radiations and molecular conduction. Abdou [23] and Badr [24] derive the solution as a series of Legendre polynomials, while Frankel in his 1995 paper [25] derives the solution of an equation of the type (23) as a series of Chebyshev polynomials. It should be noted that while Frankel considers some numerical experiments, he does not study the convergence of the obtained infinite system of linear algebraic equations. Various numerical approaches to solving equations of a similar type were considered in [26, 27].

We take an approach similar to that of Frankel [25] to reduce (23) to an infinite system of linear equations. For  $\tilde{\gamma} \neq 0$  the matrix of the system is eventually diagonally dominant and its diagonal elements tend to infinity as the row/column index tends to infinity. Using these key properties and theorems by Farid [28, Theorem 2.1] and Farid and Lancaster [29, Theorem 2.2], one can show that the matrix of the system is invertible and is a compact operator from  $l_1$  into  $l_1$ , and that the solutions of the truncated systems converge to the solution of the infinite system.

**4.1.1. Numerical Experiments**

In Table 1 the values at the crack tip of  $u_{2,1}(x, 0)$ , obtained using the method described above, are compared for various values of the (non-dimensionalized) far-field loading parameter  $\sigma$  and surface tension  $\tilde{\gamma}$ . One can observe that the larger the value of the surface excess property, the smaller the slope of the crack profile at the crack tip.

From the numerical experiments (Figures 4 and 5) it is clear that the solution  $u_2(x, 0)$  for the crack profile is a monotonically increasing function on  $(-1, 0)$  and monotonically decreasing on  $(0, 1)$ . Furthermore, the slope of the crack profile at the crack tip increases

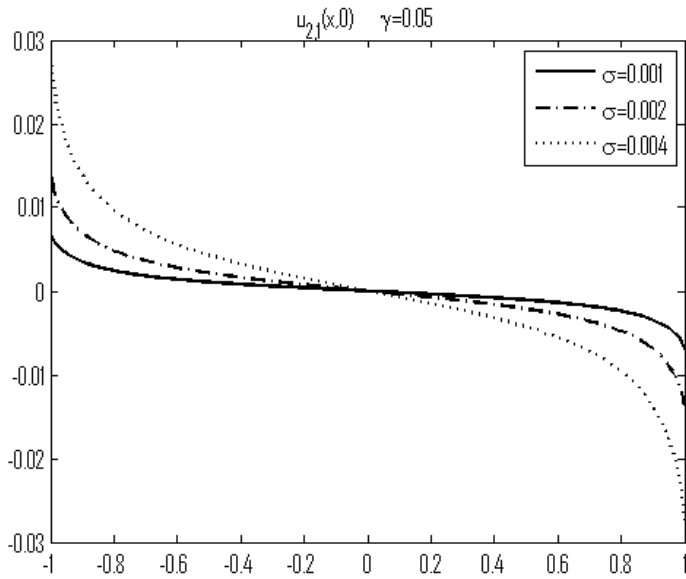


Figure 4. Approximation of  $u_{2,1}(x, 0)$  by a finite sum of Chebyshev polynomials (400 terms) for  $\tilde{\gamma} = 0.05$  and far-field loading  $\sigma = 0.001, 0.002,$  and  $0.004$ .

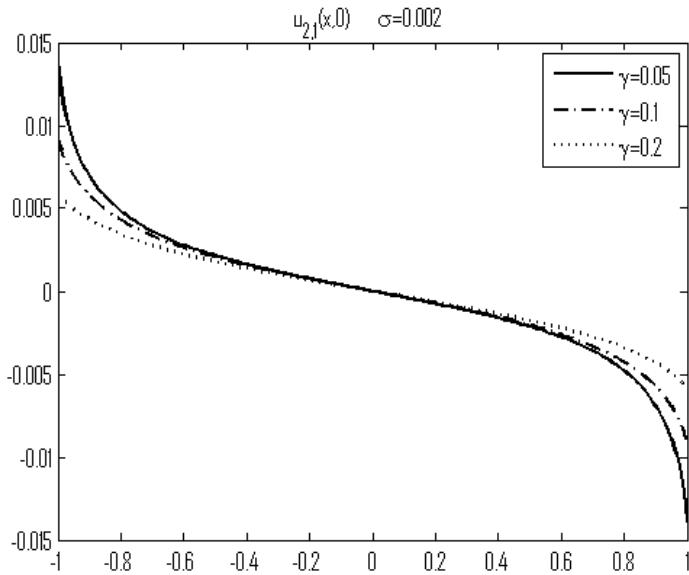


Figure 5. Approximation of  $u_{2,1}(x, 0)$  by a finite sum of Chebyshev polynomials (400 terms) for far-field loading  $\sigma_0 = 0.002$  and  $\tilde{\gamma} = 0.005, 0.01,$  and  $0.02$ .

with an increase in the far-field loading. In addition, the surface excess property  $\tilde{\gamma}$ , with the appropriate boundary condition, given by the jump momentum balance leads to a finite opening angle at the crack tip. However, (23) implies that if the crack surfaces do not come together at a cusp, i.e.  $\phi(\pm 1) = u_{2,1}(\pm 1, 0)$  is non-zero, then  $\phi'(x) = u_{2,11}(x, 0)$  has a logarithmic singularity at the crack tips. Using (17) one concludes that this leads to a logarithmically singular stress at the crack tip. This is an improvement from the classical LEFM model which leads to a square-root singularity of the crack tip stress, however, as in LEFM, any singular stress is inconsistent with the assumptions made to linearize the equations and derive (23).

**4.2. Model with Curvature Dependence in the Surface Tension and Zero Mutual Body Force Term**

In this section, as a next step, we study a model in which the mutual body force is assumed to be zero but we allow for curvature dependence in the excess property  $\tilde{\gamma}$  of the fracture surface, i.e.

$$\tilde{\gamma} = \tilde{\gamma}(H). \tag{24}$$

Even though curvature-dependent surface tension models are not common in the fracture literature, the effect of curvature-dependent surface tension has been widely studied in the context of nucleation theory [30–32].

Assuming that stresses and strains remain small and combining (85) and (24) one derives the following asymptotic expansion for  $\tilde{\gamma}$ :

$$\tilde{\gamma}(x) = \gamma_0 + \gamma_1 u_{2,11}(x, 0) + \text{h.o.t.} \tag{25}$$

where  $\gamma_0 \equiv \text{const}$  and  $\gamma_1 \equiv \text{const}$ . After substituting (25) into (10) and linearizing the jump momentum balance equations under the assumption that  $u_{i,j}(x, 0)$  and  $u_{i,jk}(x, 0)$ ,  $i, j, k = 1, 2$  are small, we obtain

$$\begin{aligned} \sigma_{12}(x, 0) &= \gamma_1 u_{2,111}(x, 0) + \text{h.o.t.} \\ \sigma_{22}(x, 0) &= -\gamma_0 u_{2,11}(x, 0) + \text{h.o.t.} \end{aligned} \tag{26}$$

Note that, unlike in the case of constant surface tension, here the shear stress on the crack surfaces to first order is not identically zero.

We proceed in a similar way to the approach taken in the case of constant  $\tilde{\gamma}$  (Section 4.1). Using (16) and splitting the displacement vector into  $\mathbf{u}_\kappa = \mathbf{u}^0 + \mathbf{u}^f$ , where the components of  $\mathbf{u}^f$  are given by (19), we arrive at the following linear integro-differential equation for  $\phi(x) = u_{2,1}^0(x, 0) = u_{2,1}(x, 0)$ :

$$\gamma_0 \phi'(x) + \frac{1}{\pi} \int_{-1}^1 \frac{\zeta_1 \phi(r) + \zeta_2 \gamma_1 \phi''(r)}{r - x} dr = -\sigma, \quad x \in (-1, 1) \tag{27}$$

where

$$\zeta_1 = \frac{E}{2(1 - \nu^2)} \quad \text{and} \quad \zeta_2 = \frac{1 - 2\nu}{2(1 - \nu)}.$$

First note that unlike in the case with  $\tilde{\gamma} \equiv \text{const}$  (cf. (23)), Equation (27) cannot have a solution  $\phi(x)$ , such that  $\phi'(x)$  is singular at the endpoints. The reason being that this would imply  $\phi''(x) \notin L^1([-1, 1])$  and consequently the Cauchy principal value integral in (27) would not exist. In turn, this implies that every solution  $\phi(x)$  of (27) satisfies

$$\zeta_1 \phi(\pm 1) + \zeta_2 \gamma_1 \phi''(\pm 1) = 0. \tag{28}$$

Thus, the solution  $\phi(x)$  ‘adjusts itself’ so that (28) is satisfied. Note that (28) cannot be viewed as a boundary condition.

Further, taking into account (11)<sub>1</sub> we look for a solution of (27) subject to

$$\phi(-1) = \phi(1) = 0 \tag{29}$$

so that  $u_{2,1}(x, 0)$  is continuous at the crack tips. Furthermore, the symmetry of the problem requires that the crack profile  $u_2(x, 0)$  be an even function of  $x$  and therefore we look for a solution  $\phi$  of (27) such that

$$\phi(x) = -\phi(-x), \quad x \in (-1, 1). \tag{30}$$

**Theorem 1.** *Problem (27), subject to (29) and (30), has a unique solution for all, apart from countably many, values of the parameters  $\gamma_0$  and  $\gamma_1$ .*

**Proof.** We use a technique introduced by Mikhlin and Prössdorf [33, Chapter VII] to reduce (27) to canonical form.

Let  $\psi(x) := \phi''(x)$ . Then

$$\phi'(x) = \int_{-1}^1 \omega_0(x, r) \psi(r) dr + c_1 \tag{31}$$

and

$$\phi(x) = \int_{-1}^1 \omega_1(x, r) \psi(r) dr + c_1(x + 1) + c_2 \tag{32}$$

where

$$\omega_0(x, r) = \begin{cases} 1, & r \in (-1, x) \\ 0, & r \in (x, 1) \end{cases}, \quad \omega_1(x, r) = \int_{-1}^1 \omega_0(x, t) \omega_0(t, r) dt$$

and  $c_1 = \phi'(-1)$ ,  $c_2 = \phi(-1)$ . After substituting (31) and (32) into (27) we arrive at a singular integral equation for  $\psi(x)$  of the form

$$\frac{\gamma_1 \zeta_2}{\pi} \int_{-1}^1 \frac{\psi(r)}{r-x} dr + \int_{-1}^1 k(x, r) \psi(r) dr = -\sigma - \gamma_0 c_1 - \frac{\zeta_1}{\pi} \int_{-1}^1 \frac{c_1(r+1) + c_2}{r-x} dr \quad (33)$$

where

$$k(x, r) = \gamma_0 \omega_0(x, r) + \frac{\zeta_1}{\pi} \int_{-1}^1 \frac{\omega_1(t, r)}{t-x} dt.$$

Using the boundary conditions (29), we obtain  $c_2 = 0$ . Also, combining (29), (30), and (31) we find

$$0 = \int_0^1 \phi'(x) dx = \int_0^1 \int_{-1}^1 \omega_0(x, r) \psi(r) dr dx + c_1. \quad (34)$$

Thus, using (29) and (30), (33) can be written in the (canonical) form

$$R[\psi](x) := \frac{\gamma_1 \zeta_2}{\pi} \int_{-1}^1 \frac{\psi(r)}{r-x} dr + \int_{-1}^1 \tilde{k}(x, r) \psi(r) dr = -\sigma \quad (35)$$

where

$$\begin{aligned} \tilde{k}(x, r) &= \gamma_0 \omega_0(x, r) + \frac{\zeta_1}{\pi} \int_{-1}^1 \frac{\omega_1(t, r)}{t-x} dt - \gamma_0 \int_0^1 \omega_0(t, r) dt \\ &\quad - \frac{\zeta_1}{\pi} \int_{-1}^1 \int_0^1 \omega_0(s, r) \frac{t+1}{t-x} ds dt. \end{aligned}$$

Let  $L^2_\varrho([-1, 1])$  denote the weighted space of functions having a finite norm

$$\|v\|_\varrho = \left( \int_{-1}^1 (1-x^2)^{1/2} |v(x)|^2 dx \right)^{1/2}.$$

It is well known [27, 33, 34] that the singular integral operator  $R[\psi]$  is a Fredholm operator from  $L^2_\varrho([-1, 1])$  to  $L^2_\varrho([-1, 1])$  of index 1. The index depends only on the dominant part of the operator: the singular integral operator

$$R_1[\psi](x) := \frac{1}{\pi} \int_{-1}^1 \frac{\psi(r)}{r-x} dr$$

and is independent of any compact perturbation, in particular, it is independent of

$$R_2[\psi](x) := \int_{-1}^1 \tilde{k}(x, r) \psi(r) dr.$$

One can show [35] that the general solution of the singular integral equation

$$g(x) = \frac{1}{\pi} \int_{-1}^1 \frac{f(r)}{r-x} dr \tag{36}$$

is given by

$$f(x) = -\frac{1}{\sqrt{1-x^2}} \left( \frac{1}{\pi} \int_{-1}^1 g(r) \frac{\sqrt{1-r^2}}{r-x} dr + C \right). \tag{37}$$

In essence, formula (37) gives an inverse of the finite Hilbert transform operator (36). Using this, we conclude that  $R_1[\psi](x)$ , restricted to the space of functions  $\psi$  with  $\int_{-1}^1 \psi(x) dx = 0$ , has a trivial null space. Therefore, (35) is equivalent to

$$\gamma_1 \zeta_2 \psi(x) + R_1^{-1} R_2[\psi](x) = R_1^{-1}[\sigma](x)$$

Note that  $R_1^{-1} R_2$  is a compact operator, being the composition of a compact with a continuous operator, and, consequently, it has a countable spectrum. Furthermore,  $\gamma_1 \zeta_2 I + R_1^{-1} R_2$ , where  $I$  is the identity operator, is invertible, unless  $-\gamma_1 \zeta_2$  is in the spectrum of  $R_1^{-1} R_2$ . This concludes the proof. □

**4.2.1. Numerical Experiments**

To find a numerical solution to problem (27), subject to (29) and (30), we employ a *spline collocation method*, similar to the one introduced by Samoïlova in [36], where a first-order singular integro-differential equation (SIDE) is solved. Spline collocation methods for SIDES were considered by many others, including Schmidt [37]. Using (30), it suffices to solve the problem on  $(0, 1)$ . Further, the boundary conditions (29) combined with (28) imply that  $\phi(1) = \phi''(1) = 0$  and (30) yields  $\phi(0) = \phi''(0) = 0$ . Consequently we can use a natural cubic spline  $S(x)$  to approximate the solution  $\phi(x)$ . Let  $0 = x_1 < x_2 < \dots < x_{N+1} = 1$  be the evenly spaced spline nodes, i.e.

$$S(x) = \begin{cases} S_1(x), & x \in [x_1, x_2] \\ S_2(x), & x \in [x_2, x_3] \\ \vdots \\ S_N(x), & x \in [x_N, x_{N+1}] \end{cases}$$

with [38]

$$S_i(x) = \frac{z_{i+1}(x-x_i)^3 + z_i(x_{i+1}-x)^3}{6h} + \left( \frac{y_{i+1}}{h} - \frac{h}{6} z_{i+1} \right) (x-x_i) + \left( \frac{y_i}{h} - \frac{h}{6} z_i \right) (x_{i+1}-x). \tag{38}$$

Here  $h = 1/N$ ,  $y_i$  approximates  $\phi(x_i)$  and the coefficients  $z_i$  can be found by solving the tridiagonal system of equations

$$\begin{aligned} z_1 &= 0 \\ z_{i-1} + 4z_i + z_{i+1} &= \frac{6}{h^2}(y_{i+1} - 2y_i + y_{i-1}) \\ z_{N+1} &= 0. \end{aligned}$$

Using (30), we transform (27) into

$$\gamma_0 \phi'(x) + \frac{2}{\pi} \int_0^1 \frac{(\zeta_1 \phi(r) + \zeta_2 \gamma_1 \phi''(r))r}{r^2 - x^2} dr = -\sigma, \quad x \in (0, 1). \tag{39}$$

The Cauchy principal value integral is calculated with the help of a *product integration method* [39, 40], i.e.

$$\int_0^1 \frac{(\zeta_1 S(r) + \zeta_2 \gamma_1 S''(r))r}{r^2 - x^2} dr = \sum_{i=1}^N \int_{x_i}^{x_{i+1}} \frac{(\zeta_1 S_i(r) + \zeta_2 \gamma_1 S''_i(r))r}{r^2 - x^2} dr,$$

and, using (38), each of the integrals on  $[x_i, x_{i+1}]$  is evaluated exactly.

In the end, the following  $(N - 1) \times (N - 1)$  linear system of equations for the unknowns  $y_2, y_3, \dots, y_N$  is solved

$$\gamma_0 S'_i(t_i) + \sum_{j=1}^N \int_{x_j}^{x_{j+1}} \frac{(\zeta_1 S_j(r) + \zeta_2 \gamma_1 S''_j(r))r}{r^2 - t_i^2} dr = -\sigma, \quad i = 2, \dots, N \tag{40}$$

where  $t_i$  is the midpoint of the interval  $[x_i, x_{i+1}]$ .

Figures 6–9 are graphs of the slope of the crack profile  $u_{2,1}(x, 0)$  and of  $\gamma_1 u_{2,11}(x, 0)$  for  $\nu = 0.33$  and various values of the parameters  $\gamma_0, \gamma_1$  and the far-field loading  $\sigma$ . Note that the parameters are non-dimensionalized (e.g.  $\zeta_1^* = \zeta_1/E$ ), but for simplicity of notation the superscript  $\star$  is dropped.

From the numerical experiments (Figure 6) it is clear that  $|\sigma_{22}(1, 0)|$ , the stress at the crack tip (in absolute value), is an increasing function of the far-field loading (cf. (26)). Furthermore, the larger the value of  $\gamma_1$ , the smaller the crack tip stress (Figure 7). Interestingly, unlike in the constant surface tension model (Section 4.1), the crack tip stress is an *increasing function* of  $\gamma_0$  (Figure 8). In Table 2 the values at the crack tip of  $\phi'(x) = u_{2,11}(x, 0)$ , in the case of curvature-dependent surface tension, are compared for various values of the (non-dimensionalized) far-field loading parameter  $\sigma$  and the parameters  $\gamma_0$  and  $\gamma_1$  which determine the surface excess property  $\tilde{\gamma}(x)$ .

It should be noted here that for certain values of the parameters, namely when  $\gamma_0$  is not much smaller than  $\gamma_1$ , the model yields unphysical solutions and predicts interpenetration of the upper and lower crack surfaces (Figure 9).

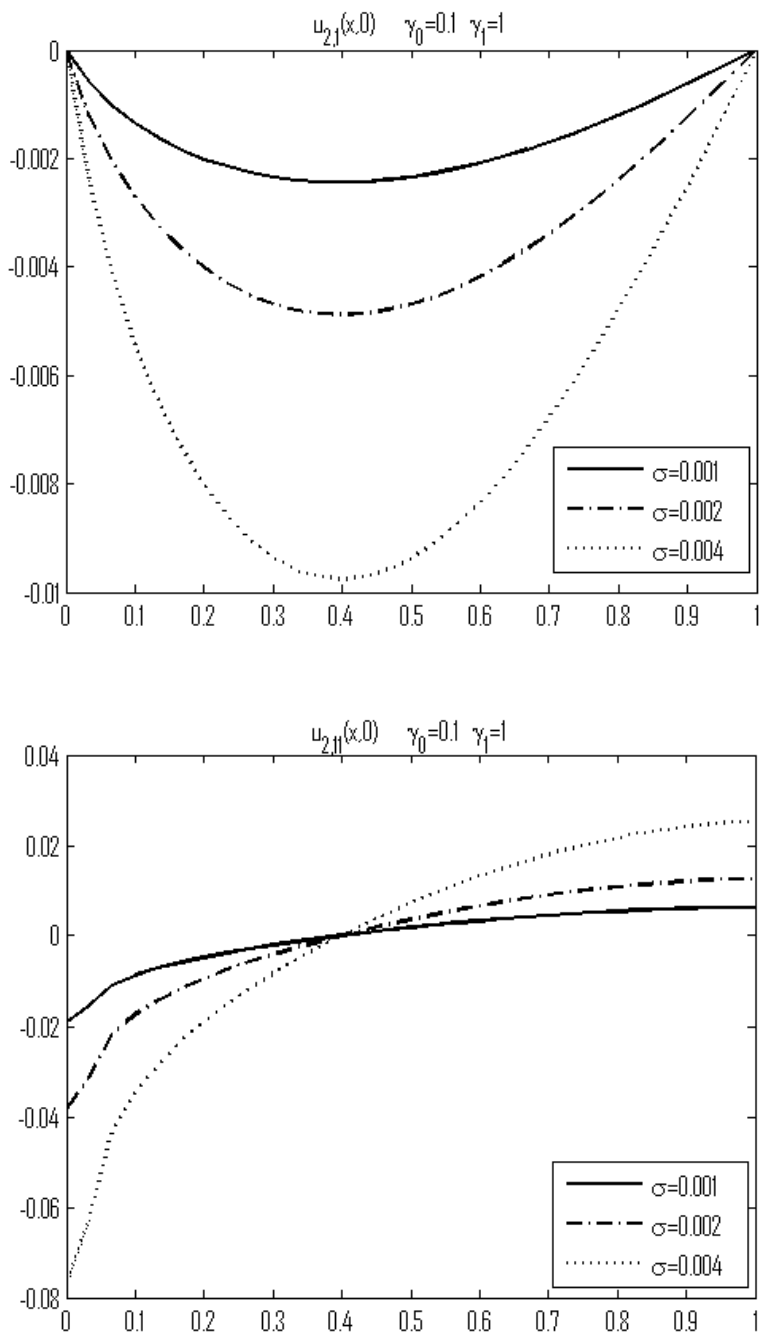


Figure 6. Graph of  $u_{2,1}(x, 0)$  and of  $\gamma_1 u_{2,11}(x, 0)$  for  $\gamma_0 = 0.1$ ,  $\gamma_1 = 1$  and far-field loading  $\sigma = 0.001, 0.002, 0.004$ .

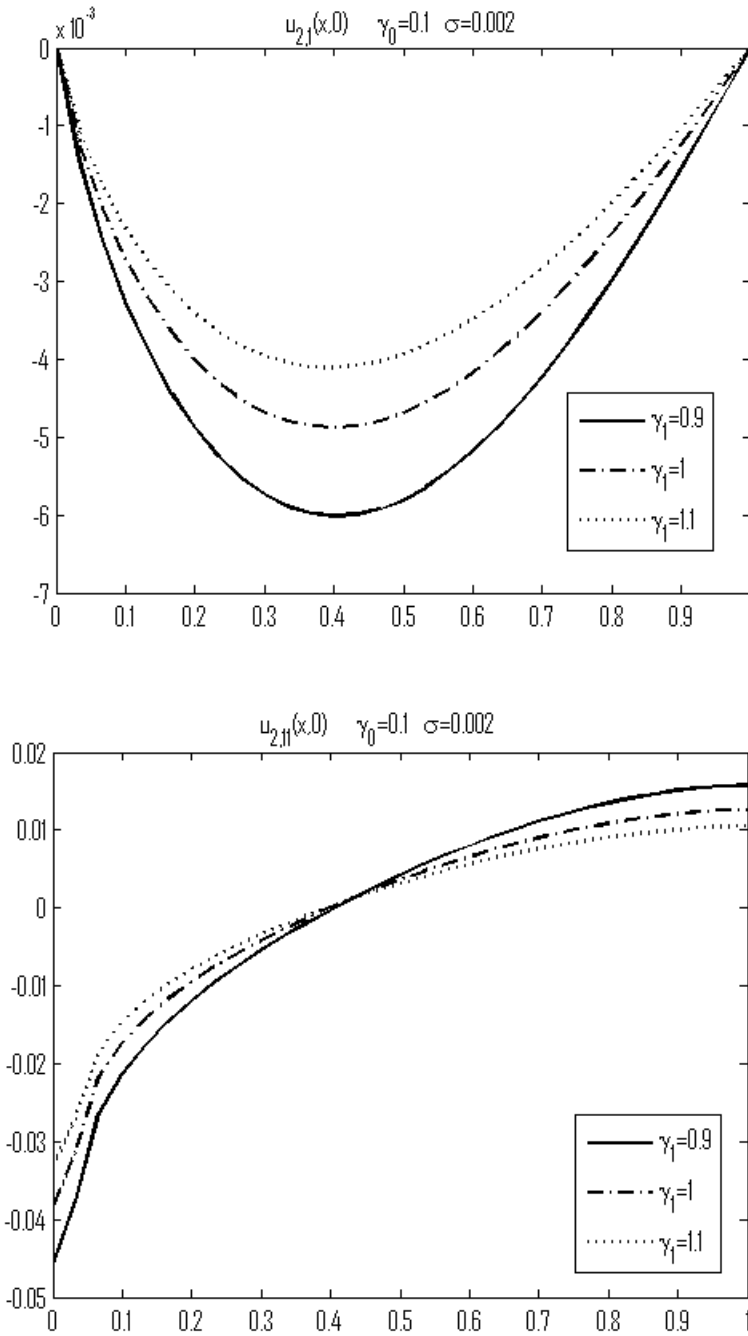


Figure 7. Graph of  $u_{2,1}(x,0)$  and of  $\gamma_1 u_{2,11}(x,0)$  for  $\gamma_0 = 0.1$ , far-field loading  $\sigma = 0.002$  and  $\gamma_1 = 0.9, 1, 1.1$ .

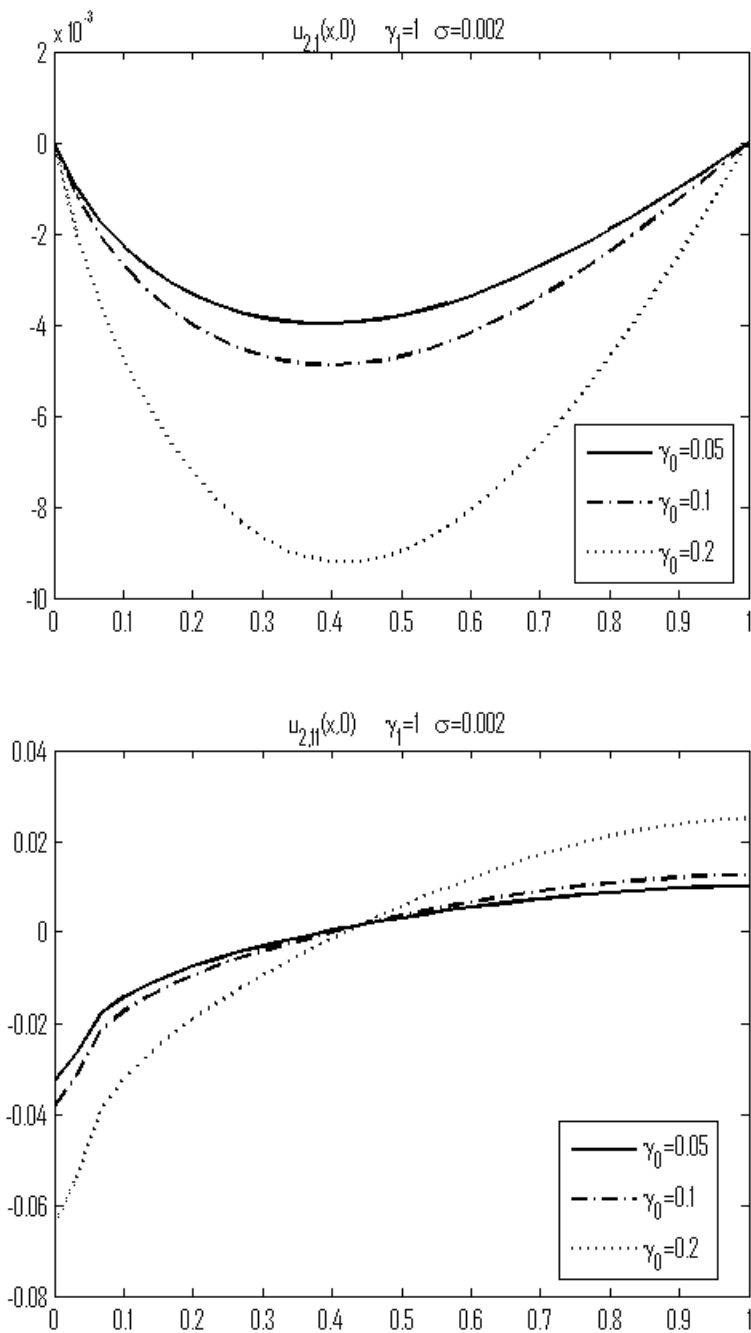


Figure 8. Graph of  $u_{2,1}(x, 0)$  and of  $\gamma_1 u_{2,11}(x, 0)$  for  $\gamma_1 = 1$ , far-field loading  $\sigma = 0.002$  and  $\gamma_0 = 0.05, 0.1, 0.2$ .

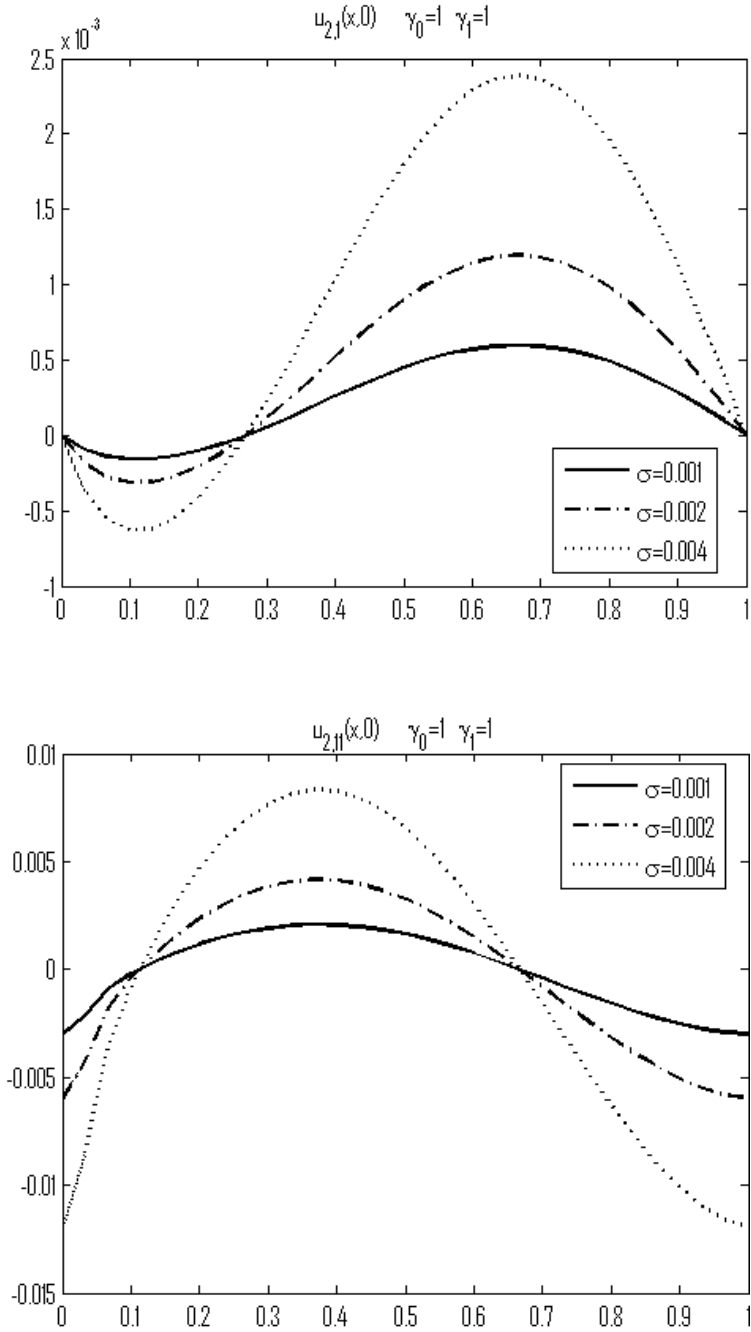


Figure 9. Graph of  $u_{2,1}(x, 0)$  and of  $\gamma_1 u_{2,11}(x, 0)$  for  $\gamma_0 = 0.1$ ,  $\gamma_1 = 1$  and far-field loading  $\sigma = 0.001, 0.002, 0.004$ .

Table 2. Value of  $\phi'(1) = u_{2,11}(1, 0)$  for various values of the (non-dimensional) far-field loading  $\sigma$  and (non-dimensionalized)  $\gamma_0$  and  $\gamma_1$ .

$\gamma_0$	$\gamma_1$	$\sigma$	$\phi'(1)$	$\gamma_0$	$\gamma_1$	$\sigma$	$\phi'(1)$	$\gamma_0$	$\gamma_1$	$\sigma$	$\phi'(1)$
0.05	0.9	0.001	0.0060	0.1	0.9	0.001	0.0079	0.2	0.9	0.001	0.0202
		0.002	0.0120			0.002	0.0158			0.002	0.0404
		0.004	0.0240			0.004	0.0315			0.004	0.0808
	1	0.001	0.0050		1	0.001	0.0063		1	0.001	0.0125
		0.002	0.0101			0.002	0.0126			0.002	0.0250
		0.004	0.0201			0.004	0.0252			0.004	0.0500
	1.1	0.001	0.0043		1.1	0.001	0.0053		1.1	0.001	0.0090
		0.002	0.0087			0.002	0.0105			0.002	0.0180
		0.004	0.0173			0.004	0.0210			0.004	0.0361

Further, models for which  $\gamma_0$  is much larger than  $\gamma_1$  predict highly oscillatory solutions. Thus, physically realistic solutions require that the dependence of surface tension upon curvature not be too weak relative to its baseline value in the limit as crack surface curvature vanishes.

Most importantly, introducing curvature dependence into the surface tension removes the crack tip stress singularity and leads to a crack profile such that the two crack surfaces meet at a cusp at the crack tip. Moreover, models with curvature-dependent surface tension yield solutions such that  $u_{2,1}(x, 0)$  and  $u_{2,11}(x, 0)$  remain small (when  $\sigma$  is small enough), which is consistent with the assumptions made to derive (27).

### 4.3. Model Including Mutual Body Force Correction

In order to construct the Dirichlet-to-Neumann (99) and the Neumann-to-Dirichlet (101) maps for the model with non-zero mutual body force correction, one needs to find a particular solution of (91), which can be done using standard techniques.

We take an approach similar to that presented in Sections 4.1 and 4.2. Specifically, using the Dirichlet-to-Neumann map (99), the Neumann-to-Dirichlet map (101) and the boundary conditions on the crack surfaces, we construct an equation relating the tensile stress  $\sigma_{22}(x, 0)$  and the slope of the crack profile  $u_{2,1}(x, 0)$  for  $x \in [-1, 1]$ , after which we linearize the components of the body force term  $\mathbf{b}_\kappa(x, t)$  under the assumption that  $u_{i,j}(x, 0)$  and  $u_{i,jk}(x, 0)$  are small.

We adopt a model for the mutual body force term analogous to the model proposed by Oh et al. [21], where the body force in the current configuration is given by  $\mathbf{b} = -\text{grad}\Phi$  with  $\Phi(x_1, x_2)$ , a correction potential of the form

$$\Phi(x_1, x_2) = \int_{-1}^1 \int_{-h(a)}^{h(a)} \int_{-\infty}^{\infty} \varphi(\sqrt{(x_1 - a)^2 + (x_2 - b)^2 + c^2}) dc db da. \quad (41)$$

Here  $\varphi$  is an interatomic potential, for example of Morse or Lennard–Jones type.<sup>6</sup>

**4.3.1. Model with Constant Surface Tension and a Mutual Body Force Term**

First consider the case where the surface excess property  $\tilde{\gamma}$  is a constant. As in Section 4.1, we split  $\mathbf{u}_\kappa = \mathbf{u}^0 + \mathbf{u}^f$  where  $\mathbf{u}^f$  is the displacement field corresponding to the homogeneous stress field determined by the far-field loading  $\sigma$ .

One can show that introducing a mutual body force term, based on a correction potential as given in (41), leads to the addition of a compact operator to the original singular integro-differential operator. More precisely, proceeding in the same way as for the derivation of (21), after linearization of the body force in the reference configuration  $\mathbf{b}_\kappa$  under the assumption of small displacement gradient, one concludes that  $u_{2,1}^0(x, 0)$  satisfies

$$-\sigma - \tilde{\gamma}u_{2,1}^0(x, 0) = \frac{E}{2(1 - \nu^2)\pi} \int_{-1}^1 \frac{u_{2,1}^0(r, 0)}{r - x} dr + \mathcal{K}[u_{2,1}^0](x) \tag{42}$$

where

$$\mathcal{K}[u_{2,1}^0](x) = \int_{-1}^1 \int_{-1}^a u_{2,1}^0(r, 0) dr K(x, a) da \tag{43}$$

with  $K : [-1, 1] \times [-1, 1] \rightarrow \mathbb{R}$  - a continuous function. Therefore,  $\mathcal{K}$  is a compact operator on  $C[-1, 1]$ , being the composition of a Fredholm integral operator of the first kind [41, p. 55] and a bounded operator on  $C[-1, 1]$ .

Let

$$\phi(x) := u_{2,1}^0(x, 0)$$

and let the singular integro-differential operator  $\mathcal{S}$  be defined by

$$\mathcal{S}[\phi](x) := \tilde{\gamma}\phi'(x) + \frac{E}{2(1 - \nu^2)\pi} \int_{-1}^1 \frac{\phi(r)}{r - x} dr.$$

Then (42) is equivalent to

$$\mathcal{S}[\phi](x) + \mathcal{K}[\phi](x) = -\sigma. \tag{44}$$

**4.3.2. Model with Curvature-dependent Surface Tension and a Mutual Body Force Term**

In the case when the surface excess property is curvature-dependent and the model includes a body force correction term, after linearizing the differential and jump momentum balances, using arguments similar to those given in the previous section, it is straightforward to show that  $u_{2,1}^0(x, 0)$  satisfies the following equation

$$\gamma_0 u_{2,1}^0(x, 0) + \frac{1}{\pi} \int_{-1}^1 \frac{\zeta_1 u_{2,1}^0(r, 0) + \zeta_2 \gamma_1 u_{2,11}^0(r, 0)}{r - x} dr + \mathcal{K}[u_{2,1}^0](x) = -\sigma. \tag{45}$$

Let

$$\tilde{S}[\phi](x) := \gamma_0 u_{2,11}^0(x, 0) + \frac{1}{\pi} \int_{-1}^1 \frac{\zeta_1 u_{2,1}^0(r, 0) + \zeta_2 \gamma_1 u_{2,11}^0(r, 0)}{r - x} dr.$$

Here the notation introduced in Section 4.2 is used. Then (45) can be written in the form

$$\tilde{S}[\phi](x) + \mathcal{K}[\phi](x) = -\sigma. \quad (46)$$

### 4.3.3. Discussion

We conjecture that if  $\tilde{\gamma} = 0$ , then for any physically reasonable correction potential the solution  $\phi$  of the singular integral equation (44) exhibits a square root singularity at the crack tip. Furthermore, if  $\tilde{\gamma}(x) \approx \gamma_0 + \gamma_1 u_{2,11}(x, 0)$  with  $\gamma_1 \neq 0$ , i.e. there is non-zero curvature dependent surface tension introduced as an excess property of the fracture surfaces, then (45) has a unique solution  $\phi(x) = u_{2,1}^0(x, 0)$  for all, apart from countably many values of the parameters  $\gamma_0$  and  $\gamma_1$ . Moreover,  $\phi(x)$  and  $\phi'(x)$  are bounded on  $[-1, 1]$ , i.e. the operator  $\tilde{S}[\cdot] + \mathcal{K}[\cdot]$ , where  $\mathcal{K}$  is the compact operator given by (43), behaves in a similar way to the singular integro-differential operator  $\tilde{S}[\cdot]$ .

In other words, it is the surface tension  $\tilde{\gamma}$  of the fracture surfaces, together with the appropriate fracture surface boundary conditions in the form of the jump momentum balance that is responsible for removing the square root singularities at the fracture tips, characteristic of the classical LEFM model. Moreover, including a mutual body force term in the model, after linearization of the jump momentum balance conditions, results in a compact perturbation of the SIDE. We conjecture that this compact perturbation does not affect the fundamental result, namely a model with curvature-dependent surface tension ascribed to the crack surfaces yields bounded stresses and strains for any physically reasonable body force correction. However, these are still open questions, subject to future investigation.

## 5. ENERGY-BASED CRACK GROWTH CONDITION

Various approaches to the thermodynamic analysis of fracture have been studied in the literature, with or without consideration of temperature effects. These approaches have incorporated classical singular theories with singular stresses and singular power flux into the crack tip (see Gurtin [42, 43] and Gurtin and Yatomi [44]) or with cohesive zones designed to remove the singularities (see Gurtin [45]). Others have included the notion of a *configurational force system*, with or without cohesive zone (see Gurtin and Shvartsman [16], Costanzo [46], Gurtin and Podio-Guidugli [14, 15]) or excess surface properties, with or without cohesive zone.

Separately, Gurtin and Murdoch [47, 48], Murdoch [49] and Fried and Gurtin [50] have developed a theory of elastic material surfaces, incorporating models with excess surface properties, not necessarily directed towards fracture.

The idea of ascribing excess properties to a dividing surface between two phases dates back to Gibbs. In the development of fracture theory, Griffith was the first to introduce surface excess properties in the context of solids, but he did not build it into a model of fracture in any concrete way. To the best of the authors' knowledge, the first comprehensive attempt to develop a fracture theory including excess properties was offered by Eftis and Liebowitz [51] (see also Zhang and Karihaloo [52], Van der Varst and De With [53]). Unfortunately, their development contains serious conceptual and technical flaws.

Our approach bears resemblance to several of the above modeling approaches in that it includes a detailed description of the surface excess properties. What is new in this approach is that, as shown in Section 4, curvature-dependent excess properties together with the appropriate jump momentum balance, which defines the boundary condition on the fracture surface, lead to a theory with bounded stresses and strains. Further, even though the model in which the surface tension is taken to be constant exhibits a logarithmic crack tip stress singularity, this singularity does not lead to an influx of energy into the crack tip, and therefore the theory outlined below is applicable in this case as well.

An energy-based crack growth condition is formulated, including terms similar to the classical notion of a critical ERR, defined in the setting of singular crack tip stresses and strains. Classically the ERR arises due to singular fields, whereas in the case of the modeling approach adopted here, a notion analogous to the ERR arises through a different mechanism, associated with the rate of working of the surface excess properties at the crack tip.

### 5.1. Problem Statement

Here we consider a plate, notched on one edge (two planes intersecting at a relatively large angle). The plate is undergoing dynamic, mode I fracture, the fracture having formed at the tip of the notch.

In our analysis of this problem, we make the following assumptions.

1. Temperature is independent of position and time.
2. The rates of external and mutual energy transmission, and the rate of contact energy transmission are negligible.
3. Mass transfer is negligible at all phase interfaces.
4. Pressure in the gas phase between crack surfaces is the atmospheric pressure, considered negligible when compared with the stresses generated in the system by deformation.

Owing to crack growth, in the modeling approach taken herein, we consider a continuous sequence of reference configurations (where the slit has different lengths). The mass transfer from the bulk material to the fracture edge and from the fracture edge to the fracture surface is more conveniently accounted for in the reference configuration using evolving natural configurations.<sup>7</sup>

### 5.2. Analysis

To simplify the discussion, the derivation of the crack growth condition given in Section 5.2 is in the context of a straight edge crack (in the reference configuration) in a bounded *two-*

*dimensional* body. An expression for the surface first Piola–Kirchhoff stress tensor  $\mathbf{T}_\kappa^{(\sigma)}$  is derived<sup>8</sup> in Appendix A, namely

$$\mathbf{T}_\kappa^{(\sigma)} = \frac{\|\mathbf{F}\boldsymbol{\tau}_\kappa\|}{\|\mathbf{P}_t\mathbf{F}^{-T}\mathbf{v}_\kappa\|} \mathbf{T}^{(\sigma)} \mathbf{P}_t \mathbf{F}^{-T}. \quad (47)$$

From here on,  $\mathcal{B}_t$  is assumed to be a bounded two-dimensional body. Let  $\mathcal{K}\{\mathcal{B}_t\}$  denote the kinetic energy of the body, expressed in terms of the current and the reference configuration:

$$\begin{aligned} \mathcal{K}\{\mathcal{B}_t\} &= \frac{1}{2} \int_{\mathcal{B}_t} \rho \|\mathbf{v}\|^2 dv + \frac{1}{2} \int_{\partial\mathcal{B}_t} \rho^{(\sigma)} \|\mathbf{v}\|^2 da + \frac{1}{2} \rho^{(c)} \|\mathbf{v}(\mathbf{c}_t, t)\|^2 \\ &= \frac{1}{2} \int_{\mathcal{B}_\kappa(t)} \rho_\kappa \|\dot{\mathbf{x}}\|^2 dV + \frac{1}{2} \int_{\partial\mathcal{B}_\kappa(t)} \rho_\kappa^{(\sigma)} \|\dot{\mathbf{x}}\|^2 dA + \frac{1}{2} \rho_\kappa^{(c)} \|\dot{\mathbf{c}}_t\|^2 \end{aligned} \quad (48)$$

where  $\rho$  is the mass density of  $\mathcal{B}_t$ ,  $\rho^{(\sigma)}$  is the surface mass density and  $\rho^{(c)}$  is the mass density associated with the fracture tip  $\mathbf{c}_t$ . In a similar way,  $\rho_\kappa$ ,  $\rho_\kappa^{(\sigma)}$ , and  $\rho_\kappa^{(c)}$  are the mass density, surface mass density, and mass density associated with the fracture tip in the reference configuration.<sup>9</sup>

Let  $\mathcal{U}\{\mathcal{B}_t\}$  be the internal energy of  $\mathcal{B}_t$  with  $\mathcal{U}\{\mathcal{B}_t\} = \mathcal{A}\{\mathcal{B}_t\} + T\mathcal{S}\{\mathcal{B}_t\}$  where  $\mathcal{A}\{\mathcal{B}_t\}$  denotes the stored energy,  $\mathcal{S}\{\mathcal{B}_t\}$  denotes the entropy, and  $T$  denotes the constant absolute temperature. Let  $\widehat{A}$  and  $\widehat{A}^{(\sigma)}$  be respectively the Helmholtz free energy density and the surface Helmholtz free energy density per unit mass, then

$$\begin{aligned} \mathcal{A}\{\mathcal{B}_t\} &= \int_{\mathcal{B}_t} \rho \widehat{A} dv + \int_{\partial\mathcal{B}_t} \rho^{(\sigma)} \widehat{A}^{(\sigma)} da \\ &= \int_{\mathcal{B}_\kappa(t)} \rho_\kappa \widehat{A} dV + \int_{\partial\mathcal{B}_\kappa(t)} \rho_\kappa^{(\sigma)} \widehat{A}^{(\sigma)} dA. \end{aligned} \quad (49)$$

In the current model there is no free energy density associated with the crack tip, although it can easily be added, if needed. Further, let  $\mathcal{P}\{\mathcal{B}_t\}$  be the power input to the body

$$\begin{aligned} \mathcal{P}\{\mathcal{B}_t\} &= \int_{\mathcal{B}_\kappa(t)} \mathbf{b}_\kappa \cdot \dot{\mathbf{x}} dV + \mathbf{b}_\kappa^{(c)} \cdot \dot{\mathbf{c}}_t + \int_{\mathcal{S}_\kappa} \mathbf{s}_\kappa^e \cdot \dot{\mathbf{x}} dA \\ &+ 2\mathbf{T}_\kappa^{(\sigma)}(\mathbf{c}(t)) \mathbf{v}_\kappa(\mathbf{c}(t)) \cdot \mathbf{F}(\mathbf{c}(t)) \dot{\mathbf{c}}(t). \end{aligned} \quad (50)$$

Here  $\mathbf{s}_\kappa^e$  are the external tractions per unit area in the reference configuration acting on the body and  $\mathbf{b}_\kappa^{(c)}$ , as in (4), is the mutual body force acting at the crack tip. Note that  $\mathcal{P}\{\mathcal{B}_t\}$  includes the power input not only through the external force system, but also from (possible) mutual body forces and surface tractions arising from the material response of the body (through the jump momentum balance). The last term in (50) represents the rate of working of the crack surface stresses at the crack tip and it is non-zero only when there is crack

extension (only the part of the crack tip velocity which is due to crack extension (bond breaking) is taken into account, Equation (68)).

The fundamental power balance can be written in the form

$$\frac{d}{dt}\mathcal{K}\{\mathcal{B}_t\} + \frac{d}{dt}\mathcal{U}\{\mathcal{B}_t\} = \mathcal{P}\{\mathcal{B}_t\} - \mathcal{D}\{\mathcal{B}_t\} \tag{51}$$

where  $\mathcal{D}\{\mathcal{B}_t\}$  is the fracture energy dissipation rate.

The entropy inequality in the form of the Clausius–Duhem inequality (see [54, p. 728] and [55, p. 130]) in the context of assumptions 1 and 2 reduces to

$$\frac{d}{dt}T\mathcal{S}\{\mathcal{B}_t\} \geq 0. \tag{52}$$

Next, following the analysis of Gurtin and Podio-Guidugli [14], we derive the transport theorems appropriate for the current setting. It is important to keep in mind that in the setting of [14], the mechanical power flux into the crack tip is not zero due to the singular crack tip stress and strain fields, whereas here stresses and strains are bounded at the crack tip. For this reason, the transport relations needed here differ from those derived in [14, 15].

**Lemma 1 (Transport relation for a ‘bulk’ function in the reference configuration).** *Let  $\Phi(\mathbf{X}, t)$  be a field defined on  $\mathcal{B}_\kappa(t) \times \mathbb{R}^+$  which is bounded and sufficiently smooth up to the crack from either side. Then*

$$\frac{d}{dt} \int_{\mathcal{B}_\kappa(t)} \Phi = \int_{\mathcal{B}_\kappa(t)} \dot{\Phi} \tag{53}$$

where  $\dot{\Phi}$  is the material time derivative of  $\Phi$ .

**Lemma 2 (Transport relation for a function defined on a growing surface in the reference configuration).** *Consider  $\mathcal{B}_\kappa(t) \subset \mathbb{R}^2$ . Let  $\Phi^{(\sigma)}(\mathbf{X}, t)$  be a field defined on the (possibly growing) crack surface  $\Sigma_\kappa(t) \times \mathbb{R}^+$  which is bounded, and sufficiently smooth on  $(\Sigma_\kappa(t) \times \mathbb{R}^+) \setminus (\{\mathbf{c}(t)\} \times \mathbb{R}^+)$ . Then*

$$\frac{d}{dt} \int_{\partial\mathcal{B}_\kappa(t)} \Phi^{(\sigma)} = \int_{\partial\mathcal{B}_\kappa(t)} \dot{\Phi}^{(\sigma)} + 2\Phi^{(\sigma)}(\mathbf{c}(t)) \|\dot{\mathbf{c}}(t)\|. \tag{54}$$

Proofs of Lemmas 1 and 2 are provided in Appendix E.

**5.2.1. Momentum Balance Relations**

Invoking the transport theorem (which has the usual form for a bulk control volume due to the fact that stresses and strains remain bounded) and standard localization arguments, one derives the local form of the balance of linear momentum in the reference configuration

$$\rho_\kappa \ddot{\mathbf{x}} = \text{Div} \mathbf{T}_\kappa + \mathbf{b}_\kappa, \quad \mathbf{X} \in \mathcal{B}_\kappa(t) \quad (55)$$

and jump momentum balance

$$\begin{aligned} \rho_\kappa^{(\sigma)} \ddot{\mathbf{x}} &= \text{Div}_{(\sigma)} \mathbf{T}_\kappa^{(\sigma)} - \llbracket \mathbf{T}_\kappa \mathbf{N} \rrbracket, \quad \mathbf{X} \in \Sigma_\kappa(t) \\ \rho_\kappa^{(\sigma)} \ddot{\mathbf{x}} &= \text{Div}_{(\sigma)} \mathbf{T}_\kappa^{(\sigma)} - \mathbf{T}_\kappa \mathbf{N} + \mathbf{s}_\kappa^e, \quad \mathbf{X} \in \mathcal{S}_\kappa. \end{aligned} \quad (56)$$

Here  $\mathbf{N}$  is the outward unit normal. For the problem considered herein,  $\Sigma_\kappa(t) = \Sigma_\kappa(t)^+ \cup \Sigma_\kappa(t)^-$  is not just a dividing surface in the body, but rather a part of its boundary and the first equation in (56) could also be written in the form

$$\rho_\kappa^{(\sigma)} \ddot{\mathbf{x}} = \text{Div}_{(\sigma)} \mathbf{T}_\kappa^{(\sigma)} - \mathbf{T}_\kappa^\pm \mathbf{N}^\pm, \quad \mathbf{X} \in \Sigma_\kappa^\pm(t). \quad (57)$$

In addition to these, there is a momentum balance at the crack tip given by

$$\rho_\kappa^{(c)} \ddot{\mathbf{c}}_t = \mathbf{b}_\kappa^{(c)} + (\rho_\kappa^{(c)} (\dot{\mathbf{c}} \cdot \mathbf{v}_\kappa(\mathbf{c}(t))) \dot{\mathbf{c}} - \mathbf{T}_\kappa^{(\sigma)}(\mathbf{c}(t)) \mathbf{v}_\kappa(\mathbf{c}(t))) \quad (58)$$

where  $\mathbf{v}_\kappa(\mathbf{c}(t))$  is the conormal at  $\mathbf{c}(t)$  (in two-dimensional space this is the unit tangent to the fracture curve) pointing away from the fracture surface. Equation (58) is based on [22, (2.1.9-15)], stated with respect to the reference configuration and modified for the case of a propagating crack in a two-dimensional body.

### 5.2.2. Crack Growth Condition

We now proceed with a derivation of a necessary condition for crack propagation, working in the reference configuration. Substitution of (48), (49), and (50) into (51) yields

$$\begin{aligned} & \frac{d}{dt} \left( \frac{1}{2} \int_{\mathcal{B}_\kappa(t)} \rho_\kappa \|\dot{\mathbf{x}}\|^2 dV + \frac{1}{2} \int_{\partial \mathcal{B}_\kappa(t)} \rho_\kappa^{(\sigma)} \|\dot{\mathbf{x}}\|^2 dA + \frac{1}{2} \rho_\kappa^{(c)} \|\dot{\mathbf{c}}_t\|^2 \right. \\ & \left. + \int_{\mathcal{B}_\kappa(t)} \rho_\kappa \widehat{A} dV + \int_{\partial \mathcal{B}_\kappa(t)} \rho_\kappa^{(\sigma)} \widehat{A}^{(\sigma)} dA \right) \\ &= \int_{\mathcal{B}_\kappa(t)} \mathbf{b}_\kappa \cdot \dot{\mathbf{x}} dV + \mathbf{b}_\kappa^{(c)} \cdot \dot{\mathbf{c}}_t + \int_{\mathcal{S}_\kappa} \mathbf{s}_\kappa^e \cdot \dot{\mathbf{x}} dA \\ &+ 2 \mathbf{T}_\kappa^{(\sigma)}(\mathbf{c}(t)) \mathbf{v}_\kappa(\mathbf{c}(t)) \cdot \mathbf{F}(\mathbf{c}(t)) \dot{\mathbf{c}}(t) - \frac{d}{dt} T \mathcal{S}\{\mathcal{B}_t\} - \mathcal{D}\{\mathcal{B}_t\}. \end{aligned} \quad (59)$$

Lemmas 1 and 2 together with (55), (56), and (59) lead to

$$\begin{aligned}
 & 2 \left( \frac{1}{2} \rho_\kappa^{(\sigma)}(\mathbf{c}(t)) \|\dot{\mathbf{c}}_t\|^2 + \rho_\kappa^{(\sigma)}(\mathbf{c}(t)) \widehat{A}^{(\sigma)}(\mathbf{c}(t)) \right) \dot{\mathbf{c}}(t) \cdot \mathbf{v}_\kappa(\mathbf{c}(t)) \\
 & + \frac{1}{2} \frac{d\rho_\kappa^{(c)}}{dt} \|\dot{\mathbf{c}}_t\|^2 + \rho_\kappa^{(c)} \dot{\mathbf{c}}_t \cdot \dot{\mathbf{c}}_t + \int_{\mathcal{B}_\kappa(t)} \left( \text{Div} \mathbf{T}_\kappa \cdot \dot{\mathbf{x}} + \rho_\kappa \dot{\widehat{A}} \right) dV \\
 & + \int_{\partial \mathcal{B}_\kappa(t)} \left( \text{Div}_{(\sigma)} \mathbf{T}_\kappa^{(\sigma)} \cdot \dot{\mathbf{x}} - \mathbf{T}_\kappa \mathbf{N} \cdot \dot{\mathbf{x}} + \rho_\kappa^{(\sigma)} \dot{\widehat{A}}^{(\sigma)} \right) dA \\
 & = \mathbf{b}_\kappa^{(c)} \cdot \dot{\mathbf{c}}_t + 2 \mathbf{T}_\kappa^{(\sigma)}(\mathbf{c}(t)) \mathbf{v}_\kappa(\mathbf{c}(t)) \cdot \mathbf{F}(\mathbf{c}(t)) \dot{\mathbf{c}}(t) \\
 & - \frac{d}{dt} TS\{\mathcal{B}_t\} - \mathcal{D}\{\mathcal{B}_t\}. \tag{60}
 \end{aligned}$$

Use of the divergence theorem yields

$$\int_{\mathcal{B}_\kappa(t)} \text{Div} \mathbf{T}_\kappa \cdot \dot{\mathbf{x}} dV = - \int_{\mathcal{B}_\kappa(t)} \mathbf{T}_\kappa \cdot \dot{\mathbf{F}} dV + \int_{\partial \mathcal{B}_\kappa(t)} \mathbf{T}_\kappa \mathbf{N} \cdot \dot{\mathbf{x}} dS \tag{61}$$

and similarly from the surface divergence theorem (see [22, (A.6.3-7) and (2.1.9-3)])

$$\begin{aligned}
 & \int_{\partial \mathcal{B}_\kappa(t)} \text{Div}_{(\sigma)} \mathbf{T}_\kappa^{(\sigma)} \cdot \dot{\mathbf{x}} dS \\
 & = - \int_{\partial \mathcal{B}_\kappa(t)} \mathbf{T}_\kappa^{(\sigma)} \cdot \nabla_{(\sigma)} \dot{\mathbf{x}} dS + (\mathbf{T}_\kappa^{(\sigma)}(\mathbf{c}(t)) \mathbf{v}_\kappa(\mathbf{c}(t)) \cdot \dot{\mathbf{c}}_t) \\
 & = - \int_{\partial \mathcal{B}_\kappa(t)} \mathbf{T}_\kappa^{(\sigma)} \cdot \dot{\mathbf{F}} \mathbf{P}_\kappa dS + 2 \mathbf{T}_\kappa^{(\sigma)}(\mathbf{c}(t)) \mathbf{v}_\kappa(\mathbf{c}(t)) \cdot \dot{\mathbf{c}}_t \tag{62}
 \end{aligned}$$

with  $\mathbf{P}_\kappa$  the perpendicular projection operator onto  $\partial \mathcal{B}_\kappa(t)$ , where Equation (71) is used.

In virtue of (58), (61), and (62), Equation (60) reduces to

$$\begin{aligned}
 & \int_{\mathcal{B}_\kappa(t)} \left( \rho_\kappa \dot{\widehat{A}} - \mathbf{T}_\kappa \cdot \dot{\mathbf{F}} \right) dV + \int_{\partial \mathcal{B}_\kappa(t)} \left( \rho_\kappa^{(\sigma)} \dot{\widehat{A}}^{(\sigma)} - \mathbf{T}_\kappa^{(\sigma)} \cdot \dot{\mathbf{F}} \mathbf{P}_\kappa \right) dA \\
 & + \left( \rho_\kappa^{(\sigma)} \left( (\mathbf{c}(t)) \|\dot{\mathbf{c}}_t\|^2 + 2(\mathbf{c}(t)) \widehat{A}^{(\sigma)}(\mathbf{c}(t)) \right) + 2\rho_\kappa^{(c)} \dot{\mathbf{c}} \cdot \dot{\mathbf{c}}_t \right) \dot{\mathbf{c}}(t) \cdot \mathbf{v}_\kappa(\mathbf{c}(t)) \\
 & + \frac{1}{2} \frac{d\rho_\kappa^{(c)}}{dt} \|\dot{\mathbf{c}}_t\|^2 \\
 & = 2 \mathbf{T}_\kappa^{(\sigma)}(\mathbf{c}(t)) \mathbf{v}_\kappa(\mathbf{c}(t)) \cdot \mathbf{F}(\mathbf{c}(t)) \dot{\mathbf{c}}(t) - \frac{d}{dt} TS\{\mathcal{B}_t\} - \mathcal{D}\{\mathcal{B}_t\}. \tag{63}
 \end{aligned}$$

Since in any isothermal process a thermoelastic material is hyperelastic ( $\mathbf{T}_\kappa = \rho_\kappa \partial_{\mathbf{F}} \widehat{A}$ ) with free energy function equal to the stored energy [55, p. 134], we have  $\rho_\kappa \dot{\widehat{A}} = \mathbf{T}_\kappa \cdot \dot{\mathbf{F}}$ .

By assumption, the surface Cauchy stress is of the form  $\mathbf{T}^{(\sigma)} = \tilde{\gamma} \mathbf{P}_t$ . Let  $\widehat{A}^{(\sigma)}(\mathbf{X}) = \overline{A}^{(\sigma)}(\mathbf{F}(\mathbf{X})) = \widetilde{A}^{(\sigma)}(j_2)$  where  $j_2 = J \|\mathbf{F}^{-T} \mathbf{N}\|$  is the Radon–Nikodym derivative of the area measure on  $\Sigma_t$  with respect to that on  $\Sigma_\kappa(t)$  (see Proposition 1, Appendix D). Then

$$\rho_\kappa^{(\sigma)} \dot{\widehat{A}}^{(\sigma)} = \rho_\kappa^{(\sigma)} \frac{d}{dj_2} \widetilde{A}^{(\sigma)}(j_2) \partial_{\mathbf{F}} j_2 \cdot \dot{\mathbf{F}}.$$

Now,

$$\begin{aligned} \partial_{\mathbf{F}} j_2 &= \|\mathbf{F}^{-T} \mathbf{N}\| \partial_{\mathbf{F}} J + J \partial_{\mathbf{F}} \|\mathbf{F}^{-T} \mathbf{N}\| \\ &= J \|\mathbf{F}^{-T} \mathbf{N}\| \mathbf{F}^{-T} - \frac{J}{\|\mathbf{F}^{-T} \mathbf{N}\|} (\mathbf{F}^{-T} \mathbf{N} \otimes \mathbf{F}^{-T} \mathbf{N}) \mathbf{F}^{-T} \\ &= J \|\mathbf{F}^{-T} \mathbf{N}\| \mathbf{P}_t \mathbf{F}^{-T} = j_2 \mathbf{P}_t \mathbf{F}^{-T}. \end{aligned}$$

On the other hand, by Proposition 1 in Appendix D

$$\mathbf{T}_\kappa^{(\sigma)} \cdot \dot{\mathbf{F}} \mathbf{P}_\kappa = j_2 \tilde{\gamma} \mathbf{P}_t \mathbf{F}^{-T} \cdot \dot{\mathbf{F}} \mathbf{P}_\kappa = j_2 \tilde{\gamma} \mathbf{P}_t \mathbf{F}^{-T} \cdot \dot{\mathbf{F}}.$$

Since (see [22, p. 325])

$$\tilde{\gamma} = \rho_\kappa^{(\sigma)} \frac{d}{dj_2} \widetilde{A}^{(\sigma)}(j_2),$$

Equation (63) reduces to

$$\begin{aligned} &\left( \rho_\kappa^{(\sigma)} \left( \mathbf{c}(t) \|\dot{\mathbf{c}}_t\|^2 + 2\mathbf{c}(t) \widehat{A}^{(\sigma)}(\mathbf{c}(t)) \right) + 2\rho_\kappa^{(c)} \dot{\mathbf{c}} \cdot \dot{\mathbf{c}}_t \right) \dot{\mathbf{c}}(t) \cdot \mathbf{v}_\kappa(\mathbf{c}(t)) \\ &+ \frac{1}{2} \frac{d\rho_\kappa^{(c)}}{dt} \|\dot{\mathbf{c}}_t\|^2 \\ &= 2\mathbf{T}_\kappa^{(\sigma)}(\mathbf{c}(t)) \mathbf{v}_\kappa(\mathbf{c}(t)) \cdot \mathbf{F}(\mathbf{c}(t)) \dot{\mathbf{c}}(t) - \frac{d}{dt} T\mathcal{S}\{\mathcal{B}_t\} - \mathcal{D}\{\mathcal{B}_t\}. \end{aligned} \quad (64)$$

Note that the terms remaining in (64) are non-zero only when the crack starts to propagate. Using  $\mathbf{T}^{(\sigma)} = \tilde{\gamma} \mathbf{P}_t$  and the results in Appendix D, one can show that  $\mathbf{T}_\kappa^{(\sigma)} \mathbf{v}_\kappa = j \tilde{\gamma} \mathbf{v}$ , where  $j = \|\mathbf{F} \mathbf{P}_\kappa\|$ . Assuming that the kinetic energy of the crack tip is negligible and appealing to the entropy inequality, (64) reduces to

$$\rho_\kappa^{(\sigma)}(\mathbf{c}(t)) \widehat{A}^{(\sigma)}(\mathbf{c}(t)) \leq j \tilde{\gamma} \frac{\dot{\mathbf{c}}(t) \cdot \mathbf{F}^T(\mathbf{c}(t)) \mathbf{v}(\mathbf{c}_t)}{\dot{\mathbf{c}}(t) \cdot \mathbf{v}_\kappa(\mathbf{c}(t))}, \quad (65)$$

where we have used  $\dot{\mathbf{c}}(t) \cdot \mathbf{v}_\kappa(\mathbf{c}(t)) > 0$ , which holds true since  $\mathbf{v}_\kappa(\mathbf{c}(t))$  is the unit tangent to the fracture surface pointing away from it and provided the crack can only change direction at an angle smaller than  $\pi/2$ . Note that in the case of plane strain  $j = \|\mathbf{F}(\mathbf{c}(t)) \mathbf{P}_\kappa(\mathbf{c}(t))\| \equiv 1$ .

Now let  $\widehat{G}_c^{(\sigma)}$  be the critical value of the surface Gibbs free energy per unit mass, which depends only on the atomic bond strength, and let  $\gamma$  be the surface energy. Here  $\widehat{G}_c^{(\sigma)}$  can be interpreted as the energy required to break the chemical bonds [56], while  $\gamma$  – as the energy required to overcome the long-range intermolecular forces [57]. Then

$$\rho_\kappa^{(\sigma)} \widehat{A}^{(\sigma)} = \rho_\kappa^{(\sigma)} \widehat{G}_c^{(\sigma)} + \gamma. \tag{66}$$

If the crack does not change direction, i.e. if  $\mathbf{P}_\kappa(\mathbf{c}(t))\dot{\mathbf{c}}(t) = \dot{\mathbf{c}}(t)$ , using  $\mathbf{v}_\kappa = \mathbf{P}_\kappa \mathbf{F}^T \mathbf{v} / \|\mathbf{P}_\kappa \mathbf{F}^T \mathbf{v}\|$ , Equation (65) can be written in the form

$$\rho_\kappa^{(\sigma)}(\mathbf{c}(t)) \widehat{G}_c^{(\sigma)}(\mathbf{c}(t)) + \gamma(\mathbf{c}(t)) \leq \widetilde{\gamma} \|\mathbf{P}_\kappa(\mathbf{c}(t)) \mathbf{F}^T(\mathbf{c}(t)) \mathbf{v}(\mathbf{c}_t)\|. \tag{67}$$

Equation (67) gives a necessary condition for crack propagation. The left-hand side of (67) depends only on the material properties at the crack tip, while the ratio on the right-hand side is related to the deformation gradient and depends on the far-field loading. The reason we refer to (67) as a crack growth condition rather than a fracture criterion has to do with the energy dissipation  $\mathcal{D}(\mathcal{B}_t)$  and the entropy production which are not being modeled in the present discussion.

**Note:** The analysis in Section 5.2 can be performed in the current configuration, if needed, in a similar way, using the analogs of Lemmas 1 and 2 for the current configuration, as well as

$$\mathbf{v}_\kappa = \frac{\mathbf{P}_\kappa \mathbf{F}^T \mathbf{v}}{\|\mathbf{P}_\kappa \mathbf{F}^T \mathbf{v}\|}$$

and

$$\mathbf{T}^{(\sigma)} = \frac{1}{j_2} \mathbf{T}_\kappa^{(\sigma)} \mathbf{P}_\kappa \mathbf{F}^T.$$

In this case one has to be careful to distinguish the motion of the crack tip due to crack extension (bond breaking) from the motion of the crack tip due to deformation. A straightforward calculation gives

$$\begin{aligned} \dot{\mathbf{c}}_t &= \mathbf{v}(\mathbf{c}_t, t) + \mathbf{F}(\mathbf{c}(t), t) \dot{\mathbf{c}}(t) \\ &= \mathbf{v}(\mathbf{c}_t, t) + (\mathbf{I} - \text{grad } \mathbf{u}(\mathbf{c}_t, t))^{-1} \dot{\mathbf{c}}(t) \end{aligned} \tag{68}$$

in which  $\mathbf{I}$  denotes the identity tensor. It follows that

$$\dot{\mathbf{c}}(t) = (\mathbf{I} - \text{grad } \mathbf{u}(\mathbf{c}_t, t))(\dot{\mathbf{c}}_t - \mathbf{v}(\mathbf{c}_t, t)) \tag{69}$$

which gives the spatial description of the crack extension velocity. In the absence of crack extension (bond breaking),  $\dot{\mathbf{c}}(t) = \mathbf{0}$  while, in general,  $\dot{\mathbf{c}}_t \neq \mathbf{0}$ .

## 6. CRACK TIP STRESS CRITERION

Since the theory proposed herein predicts a finite crack tip stress (Section 4.2), there is an alternative fracture criterion, based on crack tip stress rather than energy. This criterion appeals to the assumption that the crack will start to propagate once the cleavage stress exceeds the stress required to overcome the short-range (chemical bonds) and long-range intermolecular forces. The critical stress for a given material can (in principle) be estimated through *ab initio* molecular dynamics calculations.

For example, for the model with curvature-dependent surface tension and no body force correction term, we estimate the tensile stress at the crack tip from (26):

$$\sigma_{22}(1, 0) = -\gamma_0 u_{2,11}(1, 0) + \text{h.o.t.}$$

Since the considered model leads to finite stresses and strains, we conclude that the cleavage stress is well defined and can be calculated using the results from Section 4.2. Thus, the crack starts to propagate once the stress at the crack tip reaches the value of the critical stress<sup>10</sup>, i.e.

$$\sigma_{22}(1, 0) \geq \frac{\sigma^{\text{crit}}}{E}.$$

This new approach to formulating a fracture criterion is very appealing with its straightforward physical interpretation and simple implementation.

## 7. CONCLUSIONS

In this paper we study several types of models arising from a new approach to modeling brittle fracture based on an extension of continuum mechanics to the nanoscale, first proposed by Slattery et al. [22] and then applied in the context of fracture by Oh et al. [21]. The main idea of the theory is to correct bulk material behavior in a neighborhood of the fracture surfaces for effects of long-range intermolecular forces from adjoining phases. This, however, leads to a non-linear, non-local boundary-value problem.

The method of integral transforms applied to the Navier equations is employed to resolve the fracture profile and tensile stress at the crack surfaces. First we consider a model of fracture which incorporates constant surface tension ascribed to the fracture surfaces and use the jump momentum balance as a boundary condition at the crack surfaces, and then show that it leads to a sharp crack profile at the crack tip (as opposed to the blunt one predicted by the classical LEFM model) and stresses which exhibit a logarithmic singularity at the crack tip.

Further, a modified model is studied in which the surface excess property includes curvature dependence. We show that this model yields bounded stresses and strains. This lends support to having a stress-based fracture criterion which amounts to a simple strength of materials argument. Moreover, in the case of the curvature-dependent surface tension model, the two fracture surfaces form a cusp at the crack tip. The resulting second-order linear SIDE

is solved numerically using spline collocation methods combined with product integration techniques.

The second part of the paper is devoted to the derivation of a crack growth condition based on the global energy balance and the second law of thermodynamics. The analysis is in the spirit of Gurtin [42, 43], Gurtin and Yatomi [44] and Gurtin and Podio-Guidugli [14, 15] with the major exception that in the theory presented herein there are no stress and strain crack tip singularities in contrast to those previous studies. For this reason, the energy-based crack growth condition developed in this paper arises in a very different way from the classical notion of ERR used in the papers cited above.

The theoretical results derived for the fracture modeling paradigm studied in this paper offer a number of potentially important benefits to practical fracture mechanics analyses. In addition, the intriguing prospect of using a CCTS fracture criterion enabled by the finite crack tip stress field predicted by the model, as shown above when one uses the jump momentum balance boundary condition on fracture surfaces along with a curvature-dependent surface tension, there is no need in finite-element calculations to employ singular elements at crack tips, cohesive zones, or process zones, all of which entail difficulties to implement efficiently and accurately. With bounded crack tip stresses and strains resulting from use of the appropriate conditions, finite-element implementation is made a relatively straightforward and simple affair.

*Acknowledgments.* The authors would like to thank Dr John Slattery and Dr Kaibin Fu for the numerous fruitful discussions. This work was supported in part by the Air Force Office of Scientific Research through Grant FA9550-06-0242 and in part by award number KUS-CI-016-04 made by King Abdullah University of Science and Technology (KAUST).

## APPENDICES

### A. SURFACE GRADIENT AND SURFACE DIVERGENCE

Let  $\phi(\mathbf{x})$  be a scalar field defined in a neighborhood of a dividing surface  $\Sigma$ ,  $\mathbf{n}$  be a unit vector normal to  $\Sigma$  and let  $\mathbf{P}$  denote the projection tensor onto the tangent space to  $\Sigma$ . Then the surface gradient of  $\phi(\mathbf{x})$  is given by (see [22, p. 632])

$$\text{grad}_{(\sigma)}\phi = \mathbf{P}\text{grad}\phi. \quad (70)$$

In a similar way, the surface gradient of a vector field  $\mathbf{v}(\mathbf{x})$  may be expressed in the following form (see [22, p. 648])

$$\text{grad}_{(\sigma)}\mathbf{v} = (\text{grad}\mathbf{v})\mathbf{P} \quad (71)$$

and consequently for the surface divergence of  $\mathbf{v}$  one obtains

$$\text{div}_{(\sigma)}\mathbf{v} = \text{tr}((\text{grad}\mathbf{v})\mathbf{P}). \quad (72)$$

As for the surface divergence of a second-order tensor field  $\mathbf{A}(\mathbf{x})$ , it can be easily shown (see [22, p. 661]) that it satisfies

$$\mathbf{c} \cdot \operatorname{div}_{(\sigma)} \mathbf{A} = \operatorname{div}_{(\sigma)} (\mathbf{A}^T \mathbf{c}) \quad (73)$$

for any constant vector  $\mathbf{c}$ . Equation (73) can be used as a definition of  $\operatorname{div}_{(\sigma)} \mathbf{A}$ . The surface divergence and surface gradient satisfy product rules analogous to the standard rules (for  $\operatorname{div}$  and  $\operatorname{grad}$ ).

**Lemma 3.** *Let  $\phi$ ,  $\mathbf{v}$ ,  $\mathbf{w}$ , and  $\mathbf{A}$  be smooth fields with  $\phi$  scalar valued,  $\mathbf{v}$  and  $\mathbf{w}$  vector valued, and  $\mathbf{A}$  tensor valued. Then*

$$\operatorname{div}_{(\sigma)} (\phi \mathbf{A}) = \mathbf{A} \operatorname{grad}_{(\sigma)} \phi + \phi \operatorname{div}_{(\sigma)} \mathbf{A} \quad (74)$$

$$\operatorname{div}_{(\sigma)} (\mathbf{v} \otimes \mathbf{w}) = \mathbf{v} \operatorname{div}_{(\sigma)} \mathbf{w} + (\operatorname{grad}_{(\sigma)} \mathbf{v}) \mathbf{w}. \quad (75)$$

For a detailed discussion of the theory of elastic material surfaces, see [22, 47–49]. We can now find an explicit expression for  $\operatorname{div}_{(\sigma)} \mathbf{T}^{(\sigma)}$ . If we assume that the surface stress  $\mathbf{T}^{(\sigma)}$  is given by  $\mathbf{T}^{(\sigma)} = \tilde{\gamma} \mathbf{P}$ , where  $\mathbf{P}$  is the projection tensor defined by

$$\mathbf{P} = \mathbf{I} - \mathbf{n} \otimes \mathbf{n} \quad (76)$$

then (74) yields

$$\operatorname{div}_{(\sigma)} \mathbf{T}^{(\sigma)} = \operatorname{grad}_{(\sigma)} \tilde{\gamma} + \tilde{\gamma} \operatorname{div}_{(\sigma)} \mathbf{P}. \quad (77)$$

Now, combining (76) and (75) one has

$$\operatorname{div}_{(\sigma)} \mathbf{P} = -\operatorname{div}_{(\sigma)} \mathbf{n} \otimes \mathbf{n} = -\mathbf{n} \operatorname{div}_{(\sigma)} \mathbf{n}. \quad (78)$$

Here we have used the fact that

$$(\operatorname{grad}_{(\sigma)} \mathbf{n}) \mathbf{n} = (\operatorname{grad} \mathbf{n}) \mathbf{P} \mathbf{n} = \mathbf{0}.$$

Let us now define the *curvature* of  $\Sigma$  by

$$H = -\frac{1}{2} \operatorname{div}_{(\sigma)} \mathbf{n}^-. \quad (79)$$

Here, in order to avoid ambiguity of the definition, we have chosen the unit normal vector  $\mathbf{n}^-$  to the fracture surface  $\Sigma$ , pointing into the bulk material. Note that  $\operatorname{div}_{(\sigma)} \mathbf{P}$  is independent of how we choose the direction of  $\mathbf{n}$ . Then we can express  $\operatorname{div}_{(\sigma)} \mathbf{P}$  in the following way

$$\operatorname{div}_{(\sigma)} \mathbf{P} = 2H \mathbf{n}^-. \quad (80)$$

Using the equivalent of (5) in the current configuration and combining (3), respectively (4), (77), and (80) one concludes that the jump momentum balance in the deformed configuration takes the form

$$\text{grad}_{(\sigma)} \tilde{\gamma} + 2\tilde{\gamma} H \mathbf{n}^- + \llbracket \mathbf{T} \rrbracket \mathbf{n}^- = \mathbf{0}. \quad (81)$$

### B. COMPONENT FORM OF THE JUMP MOMENTUM BALANCE EQUATIONS IN THE REFERENCE CONFIGURATION

From Equation (2) one concludes that the unit normal vector to  $\Sigma$  pointing into the bulk material has the following component form

$$\mathbf{n}^- = \frac{1}{\sqrt{(1 + u_{1,1})^2 + u_{2,1}^2}} \langle -u_{2,1}, 1 + u_{1,1} \rangle^T, \quad (82)$$

consequently

$$\mathbf{P} = \frac{1}{(1 + u_{1,1})^2 + u_{2,1}^2} \begin{pmatrix} (1 + u_{1,1})^2 & (1 + u_{1,1})u_{2,1} \\ (1 + u_{1,1})u_{2,1} & u_{2,1}^2 \end{pmatrix}. \quad (83)$$

Here  $u_{i,j}$  are evaluated at points  $\mathbf{X}$  on  $\Sigma_\kappa$ , i.e.  $-1 \leq X_1 \leq 1$ ,  $X_2 = 0$ . Whenever this is clear, for simplicity of notation, this dependence is suppressed.

Combining Equations (70) and (83), one arrives at the following expression for  $\text{grad}_{(\sigma)} \tilde{\gamma}$ :

$$\text{grad}_{(\sigma)} \tilde{\gamma} = \frac{\tilde{\gamma}'(x_1)}{(1 + u_{1,1})^2 + u_{2,1}^2} \langle (1 + u_{1,1})^2, (1 + u_{1,1})u_{2,1} \rangle^T. \quad (84)$$

Further, the definition of a surface divergence of a smooth vector field (72) and Equation (83) yield

$$\text{div}_{(\sigma)} \mathbf{n}^- = \frac{u_{2,1}^2 u_{1,1,2} + u_{2,1} (1 + u_{1,1}) (u_{1,1,1} - u_{2,1,2}) - (1 + u_{1,1})^2 u_{2,1,1}}{((1 + u_{1,1})^2 + u_{2,1}^2)^{3/2}}. \quad (85)$$

It only remains to evaluate the term  $J \mathbf{F}^{-T} \mathbf{N}^- \cdot \mathbf{n}^-$ . The matrix of the deformation gradient in Cartesian coordinates can be written in the following form

$$[\mathbf{F}] = \begin{pmatrix} 1 + u_{1,1} & u_{1,2} \\ u_{2,1} & 1 + u_{2,2} \end{pmatrix}.$$

Using this, the fact that  $\mathbf{N}^- = \langle 0, 1 \rangle^T$  and Equation (82) for  $\mathbf{n}^-$ , one arrives at

$$J\mathbf{F}^{-T}\mathbf{N}^- \cdot \mathbf{n}^- = \frac{(1 + u_{1,1})^2 + u_{1,2}u_{2,1}}{\sqrt{(1 + u_{1,1})^2 + u_{2,1}^2}}. \quad (86)$$

Finally, Equations (77), (78), (82), (84), and (86) together with (8) lead to the following expression for the jump momentum balance equations formulated in the reference configuration:

$$\begin{aligned} \sigma_{12} &= -\frac{(1 + u_{1,1})^2 + u_{1,2}u_{2,1}}{\sqrt{(1 + u_{1,1})^2 + u_{2,1}^2}} \left( \frac{\tilde{\gamma}'(x_1)(1 + u_{1,1})^2}{(1 + u_{1,1})^2 + u_{2,1}^2} \right. \\ &\quad \left. + \frac{\tilde{\gamma}u_{2,1}(u_{2,1}^2u_{1,1,12} + u_{2,1}(1 + u_{1,1})(u_{1,11} - u_{2,12}) - (1 + u_{1,1})^2u_{2,11})}{((1 + u_{1,1})^2 + u_{2,1}^2)^2} \right), \\ \sigma_{22} &= -\frac{(1 + u_{1,1})^2 + u_{1,2}u_{2,1}}{\sqrt{(1 + u_{1,1})^2 + u_{2,1}^2}} \left( \frac{\tilde{\gamma}'(x_1)(1 + u_{1,1})u_{2,1}}{(1 + u_{1,1})^2 + u_{2,1}^2} \right. \\ &\quad \left. - \frac{\tilde{\gamma}(1 + u_{1,1})(u_{2,1}^2u_{1,1,12} + u_{2,1}(1 + u_{1,1})(u_{1,11} - u_{2,12}) - (1 + u_{1,1})^2u_{2,11})}{((1 + u_{1,1})^2 + u_{2,1}^2)^2} \right). \quad (87) \end{aligned}$$

### C. CONSTRUCTION OF THE DIRICHLET-TO-NEUMANN AND THE NEUMANN-TO-DIRICHLET MAPS

Following [35], we proceed as follows. The component form of the differential momentum balance (7) is given by

$$\begin{aligned} \sigma_{11,1} + \sigma_{12,2} + b_{\kappa 1} &= 0 \\ \sigma_{21,1} + \sigma_{22,2} + b_{\kappa 2} &= 0 \end{aligned} \quad (88)$$

where, from Hooke's law (12),

$$\begin{aligned} \sigma_{11} &= (\lambda + 2\mu)u_{1,1} + \lambda u_{2,2} \\ \sigma_{12} &= \mu(u_{1,2} + u_{2,1}) \\ \sigma_{22} &= \lambda u_{1,1} + (\lambda + 2\mu)u_{2,2}. \end{aligned} \quad (89)$$

After substituting (89) into (88) and differentiating with respect to  $x$ , one obtains

$$\begin{aligned}
 (\lambda + 2\mu)u_{1,111} + \mu u_{1,122} + (\lambda + \mu)u_{2,112} + b_{\kappa 1,1} &= 0 \\
 (\lambda + \mu)u_{1,112} + \mu u_{2,111} + (\lambda + 2\mu)u_{2,122} + b_{\kappa 2,1} &= 0.
 \end{aligned}
 \tag{90}$$

Taking the Fourier transform of (90) with respect to  $x$  results in the following system of ordinary differential equations

$$\begin{aligned}
 \mu \frac{d^2}{dy^2} \widehat{u}_{1,1} + ip(\lambda + \mu) \frac{d}{dy} \widehat{u}_{2,1} - p^2(\lambda + 2\mu) \widehat{u}_{1,1} + ip \widehat{b}_{\kappa 1} &= 0 \\
 (\lambda + 2\mu) \frac{d^2}{dy^2} \widehat{u}_{2,1} + ip(\lambda + \mu) \frac{d}{dy} \widehat{u}_{1,1} - p^2 \mu \widehat{u}_{2,1} + ip \widehat{b}_{\kappa 2} &= 0
 \end{aligned}
 \tag{91}$$

where the Fourier transform of an integrable function  $f$  on  $\mathbb{R}$  is defined by

$$\mathcal{F}[f](p) = \widehat{f}(p) = \int_{-\infty}^{\infty} f(x) e^{-ipx} dx
 \tag{92}$$

and use is made of the property

$$\mathcal{F}[f'] = ip\mathcal{F}[f]
 \tag{93}$$

for  $f$  a continuous and piecewise smooth function such that  $f' \in L^1(\mathbb{R})$  (see [58]). System (91) is equivalent to a first-order system of ordinary differential equations

$$\mathbf{Y}' = \mathbf{A}\mathbf{Y} + \mathbf{B}
 \tag{94}$$

where

$$\begin{aligned}
 \mathbf{Y} &= \left\langle \widehat{u}_{1,1}, \widehat{u}_{2,1}, \frac{d}{dy} \widehat{u}_{1,1}, \frac{d}{dy} \widehat{u}_{2,1} \right\rangle^T \\
 \mathbf{B} &= \langle 0, 0, -ip \widehat{b}_{\kappa 1}, -ip \widehat{b}_{\kappa 2} \rangle^T
 \end{aligned}$$

and

$$\mathbf{A} = \begin{pmatrix} 0 & 0 & 1 & 0 \\ 0 & 0 & 0 & 1 \\ \frac{p^2(\lambda + 2\mu)}{\mu} & 0 & 0 & -\frac{ip(\lambda + \mu)}{\mu} \\ 0 & \frac{p^2 \mu}{\lambda + 2\mu} & -\frac{ip(\lambda + \mu)}{\lambda + 2\mu} & 0 \end{pmatrix}.$$

The general solution of the homogeneous system is

$$\begin{aligned}
 Y_{h1} &= i \left( -A_1 + \frac{\lambda + 3\mu}{p(\lambda + \mu)} A_2 \right) e^{-py} - i A_2 y e^{-py} \\
 &+ i \left( A_3 + \frac{\lambda + 3\mu}{p(\lambda + \mu)} A_4 \right) e^{py} + i A_4 y e^{py} \\
 Y_{h2} &= A_1 e^{-py} + A_2 y e^{-py} + A_3 e^{py} + A_4 y e^{py} \\
 Y_{h3} &= i \left( pA_1 - \frac{2(\lambda + 2\mu)}{\lambda + \mu} A_2 \right) e^{-py} + ipA_2 y e^{-py} \\
 &+ i \left( pA_3 + \frac{2(\lambda + 2\mu)}{\lambda + \mu} A_4 \right) e^{py} + ipA_4 y e^{py} \\
 Y_{h4} &= (-pA_1 + A_2) e^{-py} - pA_2 y e^{-py} + (pA_3 + A_4) e^{py} + pA_4 y e^{py}
 \end{aligned}$$

with  $A_i = A_i(p)$ ,  $i = 1, \dots, 4$ . Then, the general solution of (94) is given by  $\mathbf{Y} = \mathbf{Y}_h + \mathbf{P}$ , where  $\mathbf{P}(p, y) = \langle \alpha_1(p, y), \alpha_2(p, y), \alpha_3(p, y), \alpha_4(p, y) \rangle^T$  is a particular solution such that  $\lim_{y \rightarrow \infty} \mathbf{P}(p, y) = \mathbf{0}$ . Thus, the general solution of (91), defined on the upper half plane, which vanishes as  $y \rightarrow \infty$  is

$$\begin{aligned}
 \hat{u}_{1,1}(p, y) &= i \left( -\text{sgn}(p)A_1 + \frac{\lambda + 3\mu}{p(\lambda + \mu)} A_2 \right) e^{-|p|y} - i \text{sgn}(p)A_2 y e^{-|p|y} + \alpha_1(p, y) \\
 \hat{u}_{2,1}(p, y) &= A_1 e^{-|p|y} + A_2 y e^{-|p|y} + \alpha_2(p, y).
 \end{aligned} \tag{95}$$

From (93) we have

$$\begin{aligned}
 \hat{u}_{1,1}(p, y) = ip\hat{u}_1(p, y) &\Rightarrow \hat{u}_{1,2}(p, y) = -\frac{i}{p} \frac{d}{dy} \hat{u}_{1,1}(p, y) \\
 \hat{u}_{2,1}(p, y) = ip\hat{u}_2(p, y) &\Rightarrow \hat{u}_{2,2}(p, y) = -\frac{i}{p} \frac{d}{dy} \hat{u}_{2,1}(p, y).
 \end{aligned}$$

The above equations together with (89) and (95) lead to

$$\begin{aligned}
 \hat{\sigma}_{12}(p, y) &= \mu \left( -\frac{i}{p} \frac{d}{dy} \hat{u}_{1,1} + \hat{u}_{2,1} \right) \\
 &= 2\mu \left( A_1 - \frac{\lambda + 2\mu}{|p|(\lambda + \mu)} A_2 + A_2 y \right) e^{-|p|y} - \frac{i}{p} \mu \frac{d}{dy} \alpha_1(p, y) + \mu \alpha_2(p, y) \\
 \hat{\sigma}_{22}(p, y) &= \lambda \hat{u}_{1,1} - \frac{i}{p} (\lambda + 2\mu) \frac{d}{dy} \hat{u}_{2,1} \\
 &= 2\mu i \left( \text{sgn}(p)A_1 - \frac{\mu}{p(\lambda + \mu)} A_2 + \text{sgn}(p)A_2 y \right) e^{-|p|y} \\
 &+ \lambda \alpha_1(p, y) - \frac{i}{p} (\lambda + 2\mu) \frac{d}{dy} \alpha_2(p, y).
 \end{aligned} \tag{96}$$

We can solve (95) for  $A_1(p)$  and  $A_2(p)$

$$A_1(p) = \widehat{u}_{2,1}(p, 0) - \alpha_2(p, 0)$$

$$A_2(p) = -\frac{ip(\lambda + \mu)}{\lambda + 3\mu} (\widehat{u}_{1,1}(p, 0) + i\operatorname{sgn}(p)\widehat{u}_{2,1}(p, 0) - i\operatorname{sgn}(p)\alpha_2(p, 0) - \alpha_1(p, 0))$$

and substitute these into (96) to arrive at

$$\begin{aligned} \widehat{\sigma}_{12}(p, 0) &= \frac{2\mu^2}{\lambda + 3\mu} \widehat{u}_{2,1}(p, 0) + i\operatorname{sgn}(p) \frac{2\mu(\lambda + 2\mu)}{\lambda + 3\mu} (\widehat{u}_{1,1}(p, 0) - \alpha_1(p, 0)) \\ &\quad + \frac{\mu(\lambda + \mu)}{\lambda + 3\mu} \alpha_2(p, 0) - \frac{i}{p} \mu \frac{d}{dy} \alpha_1(p, 0) \\ \widehat{\sigma}_{22}(p, 0) &= -\frac{2\mu^2}{\lambda + 3\mu} \widehat{u}_{1,1}(p, 0) + i\operatorname{sgn}(p) \frac{2\mu(\lambda + 2\mu)}{\lambda + 3\mu} (\widehat{u}_{2,1}(p, 0) - \alpha_2(p, 0)) \\ &\quad + \frac{(\lambda + 2\mu)(\lambda + \mu)}{\lambda + 3\mu} \alpha_1(p, 0) - \frac{i}{p} (\lambda + 2\mu) \frac{d}{dy} \alpha_2(p, 0). \end{aligned} \tag{97}$$

Next, we apply the inverse Fourier transform to Equations (97), using

$$\mathcal{F}^{-1}[i\operatorname{sgn}(p)\widehat{f}(p)](x) = \frac{1}{\pi} \int_{-\infty}^{\infty} \frac{f(r)}{r - x} dr = \mathcal{H}[f](x). \tag{98}$$

The operator  $\mathcal{H}[f]$  defined in (98) is known as the Hilbert transform. This leads us to the so-called *Dirichlet-to-Neumann* map:

$$\begin{aligned} \sigma_{12}(x, 0) &= \frac{2\mu^2}{\lambda + 3\mu} u_{2,1}(x, 0) + \frac{2\mu(\lambda + 2\mu)}{\pi(\lambda + 3\mu)} \int_{-\infty}^{\infty} \frac{u_{1,1}(r, 0) - \check{\alpha}_1(r, 0)}{r - x} dr \\ &\quad + \frac{\mu(\lambda + \mu)}{\lambda + 3\mu} \check{\alpha}_2(x, 0) + \mu \frac{d}{dy} \int_0^x \check{\alpha}_1(s, 0) ds \\ \sigma_{22}(x, 0) &= -\frac{2\mu^2}{\lambda + 3\mu} u_{1,1}(x, 0) + \frac{2\mu(\lambda + 2\mu)}{\pi(\lambda + 3\mu)} \int_{-\infty}^{\infty} \frac{u_{2,1}(r, 0) - \check{\alpha}_2(r, 0)}{r - x} dr \\ &\quad + \frac{(\lambda + 2\mu)(\lambda + \mu)}{\lambda + 3\mu} \check{\alpha}_1(x, 0) + (\lambda + 2\mu) \frac{d}{dy} \int_0^x \check{\alpha}_2(s, 0) ds \end{aligned} \tag{99}$$

where  $\check{f} = \mathcal{F}^{-1}[f]$  denotes the inverse Fourier transform of  $f$ . In order to construct the inverse map of (99), one solves Equations (97) for  $\widehat{u}_{1,1}$  and  $\widehat{u}_{2,1}$ :

$$\begin{aligned}
 \widehat{u}_{1,1}(p, 0) &= -i \operatorname{sgn}(p) \frac{\lambda + 2\mu}{2\mu(\lambda + \mu)} (\widehat{\sigma}_{12}(p, 0) - \mu \alpha_2(p, 0)) + \frac{1}{2(\lambda + \mu)} \widehat{\sigma}_{22}(p, 0) \\
 &+ \frac{\lambda + 2\mu}{2(\lambda + \mu)} \left( \alpha_1(p, 0) + \frac{\operatorname{sgn}(p)}{p} \frac{d}{dy} \alpha_1(p, 0) + \frac{i}{p} \frac{d}{dy} \alpha_2(p, 0) \right) \\
 \widehat{u}_{2,1}(p, 0) &= -i \operatorname{sgn}(p) \frac{\lambda + 2\mu}{2\mu(\lambda + \mu)} (\widehat{\sigma}_{22}(p, 0) - \lambda \alpha_1(p, 0)) - \frac{1}{2(\lambda + \mu)} \widehat{\sigma}_{12}(p, 0) \\
 &+ \frac{2\lambda + 3\mu}{2(\lambda + \mu)} \alpha_2(p, 0) + \frac{\operatorname{sgn}(p)}{p} \frac{(\lambda + 2\mu)^2}{2\mu(\lambda + \mu)} \frac{d}{dy} \alpha_2(p, 0) \\
 &- \frac{i}{p} \frac{\mu}{2(\lambda + \mu)} \frac{d}{dy} \alpha_1(p, 0). \tag{100}
 \end{aligned}$$

After applying the inverse Fourier transform to (100) one obtains the *Neumann-to-Dirichlet* map:

$$\begin{aligned}
 u_{1,1}(x, 0) &= -\frac{\lambda + 2\mu}{2\mu(\lambda + \mu)\pi} \int_{-\infty}^{\infty} \frac{\sigma_{12}(r, 0) - \mu \check{\alpha}_2(r, 0)}{r - x} dr + \frac{1}{2(\lambda + \mu)} \sigma_{22}(x, 0) \\
 &+ \frac{\lambda + 2\mu}{2(\lambda + \mu)} \left( \check{\alpha}_1(x, 0) + \frac{1}{\pi} \frac{d}{dy} \int_{-\infty}^{\infty} \int_0^r \check{\alpha}_1(s, 0) ds \frac{dr}{r - x} \right. \\
 &\quad \left. - \frac{d}{dy} \int_0^x \check{\alpha}_2(s, 0) ds \right) \\
 u_{2,1}(x, 0) &= -\frac{\lambda + 2\mu}{2\mu(\lambda + \mu)\pi} \int_{-\infty}^{\infty} \frac{\sigma_{22}(r, 0) - \lambda \check{\alpha}_1(r, 0)}{r - x} dr - \frac{1}{2(\lambda + \mu)} \sigma_{12}(x, 0) \\
 &+ \frac{2\lambda + 3\mu}{2(\lambda + \mu)} \check{\alpha}_2(x, 0) + \frac{(\lambda + 2\mu)^2}{2\mu(\lambda + \mu)\pi} \frac{d}{dy} \int_{-\infty}^{\infty} \int_0^r \frac{\check{\alpha}_2(s, 0)}{r - x} ds dr \\
 &+ \frac{\mu}{2(\lambda + \mu)} \frac{d}{dy} \int_0^x \check{\alpha}_1(s, 0) ds. \tag{101}
 \end{aligned}$$

**D. SURFACE FIRST PIOLA–KIRCHHOFF STRESS**

For purposes of deriving an expression for the surface first Piola–Kirchhoff stress tensor, it is most natural to work in a three-dimensional setting. Thus, within this section, we assume that  $\mathcal{B}_t \subset \mathbb{R}^3$  and that  $\Sigma_t$  is a two-dimensional surface. The results derived herein are valid in the two-dimensional context as well, since the problem we consider can be viewed as a three-dimensional problem, reduced to a two-dimensional problem.

The notation introduced in Section 2 is used, with  $\mathbf{s}_\kappa$  an oriented curve in the fracture surface  $\Sigma_\kappa(t)$ , parameterized by arc length  $S \in (0, L)$ . Further, let  $ds$  and  $dS$  be small length elements in the current and reference configuration, respectively. Then

$$ds = \left\| \frac{d}{dS} \chi \circ \mathbf{s}_\kappa(S) \right\| dS = \|\mathbf{F}(\mathbf{s}_\kappa(S))\boldsymbol{\tau}_\kappa(\mathbf{s}_\kappa(S))\| dS = j dS. \quad (102)$$

Here  $j = \|\mathbf{F}\boldsymbol{\tau}_\kappa\|$  is sometimes called the Radon–Nikodym derivative of the arc length measure on  $\mathbf{s} = \chi \circ \mathbf{s}_\kappa$  with respect to that on  $\mathbf{s}_\kappa$  (see [47]).

One can show that the unit conormal to the image  $\mathbf{s}$  of the curve  $\mathbf{s}_\kappa$  in the current configuration is given by the expression

$$\mathbf{v} = \frac{\mathbf{P}_t \mathbf{F}^{-T} \mathbf{v}_\kappa}{\|\mathbf{P}_t \mathbf{F}^{-T} \mathbf{v}_\kappa\|}. \quad (103)$$

Indeed, let  $\mathbf{n}$  denote the unit normal to the surface  $\Sigma_t$ , and  $\boldsymbol{\tau}_t$  be the unit tangent to the curve  $\mathbf{s}$ . To show that  $\mathbf{v}$ , as given by (103), is conormal to  $\mathbf{s}$ , it suffices to prove that  $\mathbf{v} \cdot \mathbf{n} = 0$  and  $\mathbf{v} \cdot \boldsymbol{\tau}_t = 0$ . The first is clearly satisfied since  $\mathbf{v} \in \mathcal{T}_x$ , while  $\mathbf{n} \in \mathcal{T}_x^\perp$ . For the latter note that,  $\mathbf{P}_t = \mathbf{P}_t^T$  and  $\mathbf{P}_t \mathbf{F}\boldsymbol{\tau}_\kappa = \mathbf{F}\boldsymbol{\tau}_\kappa$ , consequently

$$\mathbf{v} \cdot \boldsymbol{\tau}_t = \frac{\mathbf{P}_t \mathbf{F}^{-T} \mathbf{v}_\kappa}{\|\mathbf{P}_t \mathbf{F}^{-T} \mathbf{v}_\kappa\|} \cdot \frac{\mathbf{F}\boldsymbol{\tau}_\kappa}{\|\mathbf{F}\boldsymbol{\tau}_\kappa\|} = \frac{\mathbf{v}_\kappa}{\|\mathbf{P}_t \mathbf{F}^{-T} \mathbf{v}_\kappa\|} \cdot \frac{\boldsymbol{\tau}_\kappa}{\|\mathbf{F}\boldsymbol{\tau}_\kappa\|} = 0.$$

The total force exerted by the material in  $\mathbf{s}^+$  (the part of  $\Sigma_t$  into which  $\mathbf{v}$  points) on the material in  $\mathbf{s}^-$  is

$$\int_{\mathbf{s}} \mathbf{T}^{(\sigma)} \mathbf{v} = \int_0^L \mathbf{T}^{(\sigma)}(\chi \circ \mathbf{s}_\kappa(S)) \frac{\mathbf{P}_t \mathbf{F}^{-T} \mathbf{v}_\kappa}{\|\mathbf{P}_t \mathbf{F}^{-T} \mathbf{v}_\kappa\|} j dS = \int_{\mathbf{s}_\kappa} \mathbf{T}_\kappa^{(\sigma)} \mathbf{v}_\kappa$$

where

$$\mathbf{T}_\kappa^{(\sigma)} = \frac{\|\mathbf{F}\boldsymbol{\tau}_\kappa\|}{\|\mathbf{P}_t \mathbf{F}^{-T} \mathbf{v}_\kappa\|} \mathbf{T}^{(\sigma)} \mathbf{P}_t \mathbf{F}^{-T} \quad (104)$$

is the surface first Piola–Kirchhoff stress tensor.<sup>11</sup>

**Proposition 1.** Let  $J = \det(\mathbf{F})$ , then

$$\frac{\|\mathbf{F}\boldsymbol{\tau}_\kappa\|}{\|\mathbf{P}_t \mathbf{F}^{-T} \mathbf{v}_\kappa\|} = J \|\mathbf{F}^{-T} \mathbf{N}\|, \quad (105)$$

in particular, (47) is independent of the conormal  $\mathbf{v}_\kappa$ . Furthermore, if  $\mathbf{n} = \mathbf{F}^{-T} \mathbf{N} / \|\mathbf{F}^{-T} \mathbf{N}\|$  (i.e.  $\mathbf{n}$  is the unit normal to  $\Sigma_t$ ) and  $da_n$  and  $dA_N$  are area elements for surfaces in the current (respectively, reference) configuration, normal to  $\mathbf{n}$  and  $\mathbf{N}$ , respectively, then

$$da_n = J \|\mathbf{F}^{-T}\mathbf{N}\| dA_N = j_2 dA_N,$$

i.e.  $j_2 = J \|\mathbf{F}^{-T}\mathbf{N}\|$  is the Radon–Nikodym derivative of the area measure on  $\Sigma_t$  with respect to that on  $\Sigma_\kappa(t)$ .

**Proof.** By the spectral theorem [59], there exists a representation of  $\mathbf{U}$  in the form

$$\mathbf{U} = \sum \alpha_i \mathbf{e}_i \otimes \mathbf{e}_i$$

where  $B = \{\mathbf{e}_i, i = 1, 2, 3\}$  is an orthonormal basis for the vector space  $\mathcal{V}$ , consisting of eigenvectors of  $\mathbf{U}$ , and  $\alpha_i$  are the corresponding eigenvalues. Let  $[\mathbf{v}_\kappa] = \langle a_\nu, b_\nu, c_\nu \rangle^T$  and  $[\mathbf{N}] = \langle a_N, b_N, c_N \rangle^T$  be the representations of  $\mathbf{v}_\kappa$  and  $\mathbf{N}$ , respectively, relative to the basis  $B$ . Recall that  $\tau_\kappa = \mathbf{N} \times \mathbf{v}_\kappa$ , therefore

$$\begin{aligned} j &= \|\mathbf{F}\tau_\kappa\| \\ &= \sqrt{\alpha_1^2(b_N c_\nu - b_\nu c_N)^2 + \alpha_2^2(c_N a_\nu - c_\nu a_N)^2 + \alpha_3^2(c_N a_\nu - c_\nu a_N)^2}. \end{aligned} \quad (106)$$

Furthermore,

$$\begin{aligned} \|\mathbf{P}_t \mathbf{F}^{-T} \mathbf{v}_\kappa\| &= \left\| \left( \mathbf{I} - \frac{\mathbf{F}^{-T} \mathbf{N} \otimes \mathbf{F}^{-T} \mathbf{N}}{\|\mathbf{F}^{-T} \mathbf{N}\|^2} \right) \mathbf{F}^{-T} \mathbf{v}_\kappa \right\| \\ &= \left\| \mathbf{U}^{-1} \mathbf{v}_\kappa - \frac{\mathbf{U}^{-2} \mathbf{N} \cdot \mathbf{v}_\kappa}{\|\mathbf{U}^{-1} \mathbf{N}\|^2} \mathbf{U}^{-1} \mathbf{N} \right\|. \end{aligned}$$

After some straightforward manipulations one concludes

$$\begin{aligned} \frac{\|\mathbf{F}\tau_\kappa\|}{\|\mathbf{P}_t \mathbf{F}^{-T} \mathbf{v}_\kappa\|} &= \sqrt{\alpha_2^2 \alpha_3^2 a_N^2 + \alpha_1^2 \alpha_3^2 b_N^2 + \alpha_1^2 \alpha_2^2 c_N^2} \\ &= \alpha_1 \alpha_2 \alpha_3 \sqrt{\frac{a_N^2}{\alpha_1^2} + \frac{b_N^2}{\alpha_2^2} + \frac{c_N^2}{\alpha_3^2}} = J \|\mathbf{F}^{-T} \mathbf{N}\|. \end{aligned}$$

Now, by Nanson's formula,

$$\mathbf{n} da_n = J \mathbf{F}^{-T} \mathbf{N} dA_N.$$

Taking the inner product of the above equation with  $\mathbf{n} = \mathbf{F}^{-T} \mathbf{N} / \|\mathbf{F}^{-T} \mathbf{N}\|$  yields

$$da_n = J \|\mathbf{F}^{-T} \mathbf{N}\| dA_N$$

which concludes the proof.  $\square$

**E. PROOFS OF LEMMAS 1 AND 2**

**Proof (Lemma 1).** Let  $\mathcal{D}_\kappa^\delta(t)$  denote a disk of radius  $\delta$  centered at the crack tip  $\mathbf{c}(t)$  and moving with it. Let  $\mathcal{B}_\kappa^\delta(t) = \mathcal{B}_\kappa(t) \setminus \mathcal{D}_\kappa^\delta(t)$ . Then

$$\frac{d}{dt} \int_{\mathcal{B}_\kappa^\delta(t)} \Phi = \int_{\mathcal{B}_\kappa^\delta(t)} \dot{\Phi} - \int_{\partial \mathcal{D}_\kappa^\delta(t)} \Phi \dot{\mathbf{c}}(t) \cdot \mathbf{N}.$$

Here  $\mathbf{N}$  is the unit normal vector to  $\partial \mathcal{D}_\kappa^\delta(t)$  pointing into the bulk material. Using the regularity and boundedness of  $\Phi$  one concludes that

$$\frac{d}{dt} \int_{\mathcal{B}_\kappa(t)} \Phi = \lim_{\delta \rightarrow 0} \frac{d}{dt} \int_{\mathcal{B}_\kappa^\delta(t)} \Phi = \int_{\mathcal{B}_\kappa(t)} \dot{\Phi}.$$

□

**Proof (Lemma 2).** Let  $l(t)$  be a curve in  $\mathbb{R}^2$  parameterized by  $\mathbf{l}(s, t)$ ,  $0 \leq s \leq 1$  with  $\mathbf{a}(t) = \mathbf{l}(0, t)$  and  $\mathbf{b}(t) = \mathbf{l}(1, t)$ . Then the standard transport theorem yields

$$\frac{d}{dt} \int_{l(t)} \Phi = \int_{l(t)} \dot{\Phi} + \Phi(\mathbf{a}(t)) \dot{\mathbf{a}} \cdot \mathbf{N}_a + \Phi(\mathbf{b}(t)) \dot{\mathbf{b}} \cdot \mathbf{N}_b$$

where  $\mathbf{N}_a$  and  $\mathbf{N}_b$  are the unit tangent vectors to  $l(t)$  at  $\mathbf{a}(t)$  and  $\mathbf{b}(t)$  respectively. Now let  $l(t) = \mathcal{S}_\kappa \cup \Sigma_\kappa(t)$ . Then  $\mathbf{a}(t) = \mathbf{b}(t) = \mathbf{c}(t)$  and  $\dot{\mathbf{a}} \cdot \mathbf{N}_a = \dot{\mathbf{b}} \cdot \mathbf{N}_b = \|\dot{\mathbf{c}}(t)\|$ , which concludes the proof. □

**NOTES**

1. An interesting exception is the recent work by Ortiz and colleagues [1–3] to derive universal forms for cohesive laws in crystalline materials. However, their studies consider the work of decohesion required to separate infinite, parallel planes of atoms in the renormalized limit of infinitely many layers of atoms. It is not clear how appropriate that is for modeling the work required to open the short (atomic-scale) cohesive zone in a brittle crystal for which the assumption of infinite parallel planes of atoms seems of dubious validity.
2. The subscript  $t$  is suppressed in the static case.
3. See Appendix A for the definitions of surface gradient and surface divergence.
4. For a derivation of the jump momentum balance in the current configuration, see Appendix A.
5. See Appendix A.
6. If the potential becomes singular as the distance between the points tends to zero, hard-sphere approximation is used.
7. An alternative approach to modeling crack propagation takes the body to be the bulk material together with the gas phase. In this case no points are ‘added’ to the boundary and thus one does not need to consider an evolving reference configuration. However, in this approach one must account for the mass transfer between the bulk material, the dividing surface, and the fracture tip. In essence, fracture propagation is viewed as a ‘chemical reaction’ occurring at the fracture edge.

8. The derivation for  $\mathbf{T}_\kappa^{(\sigma)}$  presented herein corrects a small mistake in [47] in the formula, corresponding to (103), relating the conormal in the current to the conormal in the reference configuration. For this reason, the expression for  $\mathbf{T}_\kappa^{(\sigma)}$  derived here differs slightly from the formula given in [47].
9. Owing to the fact that the upper and lower fracture surfaces meet at an angle (strictly less than  $\pi$ ), the fracture tip (in the case of three dimensions, the fracture edge) is viewed as a ‘common point’ (in the case of three dimensions, a common line), endowed with mass density.
10. Here  $\sigma_{22}$  denotes the non-dimensionalized tensile stress.
11. The formulas (103) and (104) should be compared with (5.23) and (5.24) in [47] which we believe to be in error.

## REFERENCES

- [1] Nguyen, O. and Ortiz, M. Coarse-graining and renormalization of atomistic binding relations and universal macroscopic cohesive behavior. *Journal of the Mechanics and Physics of Solids*, 50(8), 1727–1741 (2002).
- [2] Braides, A., Lew, A. J. and Ortiz, M. Effective cohesive behavior of layers of interatomic planes. *Archive for Rational Mechanics and Analysis*, 180(2), 151–182 (2006).
- [3] Hayes, R. L., Ortiz, M. and Carter, E. A. Universal binding-energy relation for crystals that accounts for surface relaxation. *Physical Review B*, 69(17), 172104 (2004).
- [4] Abraham, F. F. The atomic dynamics of fracture. *Journal of the Mechanics and Physics of Solids*, 49, 2095–2111 (2001).
- [5] Abraham, F. F., Brodbeck, D., Rudge, W. E. and Xu, X. A molecular dynamics investigation of rapid fracture mechanics. *Journal of the Mechanics and Physics of Solids*, 45(8), 1595–1619 (1997).
- [6] Abraham, F. F. and Gao, H. How fast can cracks propagate? *Physical Review Letters*, 84(14), 3113–3116 (2000).
- [7] Fineberg, J., Gross, S. P., Marder, M. and Swinney, H. L. Instability in dynamic fracture. *Physical Review Letters*, 67(4), 457–460 (1991).
- [8] Holland, D. and Marder, M. P. Ideal brittle fracture of silicon studied with molecular dynamics. *Physical Review Letters*, 80(4), 746–749 (1998).
- [9] Marder, M. and Gross, S. Origin of crack tip instabilities. *Journal of the Mechanics and Physics of Solids*, 43(1), 1–48 (1995).
- [10] Slepyan, L. I., Ayzenberg-Stepanenko, M. V. and Dempsey, J. P. A lattice model for viscoelastic fracture. *Mechanics of Time-Dependent Materials*, 3, 159–203 (1999).
- [11] Swadener, J. G., Baskes, M. I. and Nastasi, M. Molecular dynamics simulation of brittle fracture in silicon. *Physical Review Letters*, 89(8): 85503 (1–4) (2002).
- [12] Tadmor, E. B., Phillips, R. and Ortiz, M. Mixed atomistic and continuum models of deformation in solids. *Langmuir*, 12, 4529–4534 (1996).
- [13] Xiao, S. P. and Belytschko, T. A bridging domain method for coupling continua with molecular dynamics. *Computer Methods in Applied Mechanics and Engineering*, 193, 1645–1669 (2004).
- [14] Gurtin, M. E. and Podio-Guidugli, P. Configurational forces and the basic laws for crack propagation. *Journal of the Mechanics and Physics of Solids*, 44(6), 905–927 (1996).
- [15] Gurtin, M. E. and Podio-Guidugli, P. Configurational forces and a constitutive theory for crack propagation that allows for kinking and curving. *Journal of the Mechanics and Physics of Solids*, 46(8), 1343–1378 (1998).
- [16] Gurtin, M. E. and Shvartsman, M. M. Configurational forces and the dynamics of planar cracks in three-dimensional bodies. *Journal of Elasticity*, 48(2), 167–191 (1997).
- [17] Sivaloganathan, J. and Spector, S. J. On cavitation, configurational forces and implications for fracture in a nonlinearly elastic material. *Journal of Elasticity*, 67(1), 25–49 (2002).
- [18] Maugin, G. A. and Trimarco, C. Dissipation of configurational forces in defective elastic solids. *Archives of Mechanics*, 47(1), 81–99 (1995).
- [19] Fomethé, A. and Maugin, G. A. On the crack mechanics of hard ferromagnets. *International Journal of Non-Linear Mechanics*, 33(1), 85–95 (1998).
- [20] Silling, S. A. Reformulation of elasticity theory for discontinuities and long-range forces. *Journal of the Mechanics and Physics of Solids*, 48(1), 175–209 (2000).
- [21] Oh, E. S., Walton, J. R. and Slattery, J. C. A theory of fracture based upon an extension of continuum mechanics to the nanoscale. *Journal of Applied Mechanics*, 73(5), 792–798 (2006).
- [22] Slattery, J. C., Sagis, L. and Oh, E.-S. *Interfacial Transport Phenomena*, 2nd edn. Springer, Berlin, 2007.

- [23] Abdou, M. A. Fredholm-Volterra integral equation with singular kernel. *Applied Mathematics and Computation*, 137(2–3), 231–243 (2003).
- [24] Badr, A. A. Integro-differential equation with Cauchy kernel. *Journal of Computational and Applied Mathematics*, 134(1–2), 191–199 (2001).
- [25] Frankel, J. I. A Galerkin solution to a regularized Cauchy singular integro-differential equation. *Quarterly of Applied Mathematics*, 53(2), 245–258 (1995).
- [26] Atkinson, K. E. *The numerical solution of integral equations of the second kind (Cambridge Monographs on Applied and Computational Mathematics, Vol. 4)*. Cambridge University Press, Cambridge, 1997.
- [27] Saranen, J. and Vainikko, G. *Periodic integral and pseudodifferential equations with numerical approximation (Springer Monographs in Mathematics)*. Springer, Berlin, 2002.
- [28] Farid, F. O. Spectral properties of perturbed linear operators and their application to infinite matrices. *Proceedings of the American Mathematical Society*, 112(4), 1013–1022 (1991).
- [29] Farid, F. O. and Lancaster, P. Spectral properties of diagonally dominant infinite matrices. I. *Proceedings of the Royal Society Edinburgh Section A*, 111(3–4), 301–314 (1989).
- [30] Moody, M. P. and Attard, P. Curvature dependent surface tension from a simulation of a cavity in a Lennard–Jones liquid close to coexistence. *The Journal of Chemical Physics*, 115, 8967 (2001).
- [31] Moody, M. P. and Attard, P. Curvature-dependent surface tension of a growing droplet. *Physical Review Letters*, 91(5), 56104 (2003).
- [32] Schmelzer, J. W. P., Gutzow, I. and Schmelzer, J., Jr. Curvature-dependent surface tension and nucleation theory. *Journal of Colloid and Interface Science*, 178(2), 657–665 (1996).
- [33] Mikhlin, S. G. and Prössdorf, S. *Singular integral operators*. Springer, Berlin, 1986. (Translated from the German by Albrecht Böttcher and Reinhard Lehmann.)
- [34] Muskhelishvili, N. I. Boundary problems of function theory and their application to mathematical physics. *Singular integral equations*. Noordhoff International Publishing, Leyden, 1977. (Revised translation from the Russian, edited by J. R. M. Radok, Reprint of the 1958 edition.)
- [35] F. D. Gakov. *Boundary Value Problems*. Pergamon Press, London, 1966.
- [36] Samoïlova, È. N. Spline approximations of the solution of a singular integro-differential equation. *Izvestiya Vysshikh Uchebnykh Zavedenii. Matematika*, 11, 35–45 (2001).
- [37] Schmidt, G. Spline collocation for singular integro-differential equations over  $(0, 1)$ . *Numerical Mathematics*, 50(3), 337–352 (1987).
- [38] Burden, R. L., Faires, J. D. and Reynolds, A. C. *Numerical analysis*. Prindle, Weber & Schmidt, Boston, MA, 1978.
- [39] de Hoog, F. and Weiss, R. Asymptotic expansions for product integration. *Mathematics of Computation*, 27, 295–306 (1973).
- [40] Wesseling, P. An asymptotic expansion for product integration applied to Cauchy principal value integrals. *Numerical Mathematics*, 24(5), 435–442 (1975).
- [41] Zeidler, E. Fixed-point theorems. *Nonlinear functional analysis and its applications. I*. Springer-Verlag, New York, 1986. (Translated from the German by Peter R. Wadsack.)
- [42] Gurtin, M. E. On the energy release rate in quasi-static elastic crack propagation. *Journal of Elasticity*, 9(2), 187–195 (1979).
- [43] Gurtin, M. E. Thermodynamics and the Griffith criterion for brittle fracture. *International Journal of Solids and Structures*, 15, 552–560 (1979).
- [44] Gurtin, M. E. and Yatomi, C. On the energy release rate in elastodynamic crack propagation. *Archive for Rational Mechanics and Analysis*, 74(3), 231–247 (1980).
- [45] Gurtin, M. E. Thermodynamics and the cohesive zone in fracture. *Zeitschrift für Angewandte Mathematik und Physik*, 30, 991–1003 (1979).
- [46] Costanzo, F. An analysis of 3D crack propagation using cohesive zone models and the theory of configurational forces. *Mathematics and Mechanics of Solids*, 6(2), 149–173 (2001).
- [47] Gurtin, M. E. and Murdoch, A. I. A continuum theory of elastic material surfaces. *Archive for Rational Mechanics and Analysis*, 57, 291–323 (1975).
- [48] Gurtin, M. E. and Murdoch, A. I. Addenda to our paper “A continuum theory of elastic material surfaces” (Arch. Rational Mech. Anal. 57 (1975), 291–323). *Archive for Rational Mechanics and Analysis*, 59(4), 389–390 (1975).
- [49] Murdoch, A. I. A thermodynamical theory of elastic material interfaces. *Quarterly Journal of Mechanics and Applied Mathematics*, 29(3), 245–275 (1976).
- [50] Fried, E. and Gurtin, M. E. Thermomechanics of the interface between a body and its environment. *Continuum Mechanics and Thermodynamics*, 19(5), 253–271 (2007).

- [51] Eftis, J. and Liebowitz, H. On surface energy and the continuum thermodynamics of brittle fracture. *Engineering Fracture Mechanics*, 8(3), 459–485 (1976).
- [52] Zhang, C. Y. and Karihaloo, B. L. A thermodynamic framework of fracture mechanics. *Natural Science Journal of Xiangtan University*, 14(3), 148–159 (1992).
- [53] Van der Varst, P. G. T. and De With, G. Notes on the paper—a thermodynamic framework of fracture mechanics. *Engineering Fracture Mechanics*, 51(2), 333–334 (1995).
- [54] Slattery, J. C. *Interfacial Transport Phenomena*. Springer, New York, 1990.
- [55] Liu, I. S. *Continuum Mechanics*. Springer, Berlin, 2002.
- [56] Harkins, W. D. Energy relation of the surface of solids. *Journal of Chemical Physics*, 10, 268–272 (1942).
- [57] Israelachvili, J. N. *Intermolecular and surface forces*. Academic Press, London, 1991.
- [58] Folland, G. B. *Fourier analysis and its applications (The Wadsworth & Brooks/Cole Mathematics Series)*. Wadsworth & Brooks/Cole Advanced Books & Software, Pacific Grove, CA, 1992.
- [59] Gurtin, M. E. *An Introduction to Continuum Mechanics*, 1st edn. Academic Press, New York, 1981.